Cysteine Modification Alters Voltage- and Ca^{2+}-dependent Gating of Large Conductance (BK) Potassium Channels

Guangping Zhang and Frank T. Horrigan

Department of Physiology, University of Pennsylvania School of Medicine, Philadelphia, PA 19104

ABSTRACT The Ca^{2+}-activated K^+ (BK) channel α-subunit contains many cysteine residues within its large COOH-terminal tail domain. To probe the function of this domain, we examined effects of cysteine-modifying reagents on channel gating. Application of MTSET, MTSES, or NEM to mSlo1 or hSlo1 channels changed the voltage and Ca^{2+} dependence of steady-state activation. These reagents appear to modify the same cysteines but have different effects on function. MTSET increases I_K and shifts the G_K–V relation to more negative voltages, whereas MTSES and NEM shift the G_K–V in the opposite direction. Steady-state activation was altered in the presence or absence of Ca^{2+} and at negative potentials where voltage sensors are not activated. Combinations of $[Ca^{2+}]$ and voltage were also identified where P_o is not changed by cysteine modification. Interpretation of our results in terms of an allosteric model indicate that cysteine modification alters Ca^{2+} binding and the relative stability of closed and open conformations as well as the coupling of voltage sensor activation and Ca^{2+} binding and to channel opening. To identify modification-sensitive residues, we examined effects of MTS reagents on mutant channels lacking one or more cysteines. Surprisingly, the effects of MTSES on both voltage- and Ca^{2+}-dependent gating were abolished by replacing a single cysteine (C430) with alanine. C430 lies in the RCK1 (regulator of K^+ conductance) domain within a series of eight residues that is unique to BK channels. Deletion of these residues shifted the G_K–V relation by >-80 mV. Thus we have identified a region that appears to strongly influence RCK domain function, but is absent from RCK domains of known structure. C430A did not eliminate effects of MTSET on apparent Ca^{2+} affinity. However an additional mutation, C615S, in the Haem binding site reduced the effects of MTSET, consistent with a role for this region in Ca^{2+} binding.

KEY WORDS: calcium • potassium channel • BK channel • cysteine • RCK domain

INTRODUCTION

Large conductance Ca^{2+}-activated K^+ (BK) channels participate in many important physiological processes through their ability to respond to changes in membrane voltage and intracellular Ca^{2+}. Therefore, mechanisms that underlie or regulate voltage- and Ca^{2+}-dependent gating are important to understand. The pore-forming α-subunit of BK channels contains a core domain resembling that of other voltage-dependent K^+ channels with six transmembrane segments (S1–S6) including a charge S4 voltage sensor (Adelman et al., 1992; Butler et al., 1993). In addition, the channel contains a cytosolic COOH-terminal tail domain that represents almost 70% of the channel protein as well as a unique NH_2-terminal S0 transmembrane segment (Meera et al., 1997). Regions within the tail domain have been identified that influence channel activation by micromolar Ca^{2+} (Schreiber and Salkoff, 1997; Schreiber et al., 1999; Bao et al., 2002, 2004; Qian et al., 2002; Xia et al., 2002) as well as many other aspects of channel function under physiological or pathophysiological conditions, including regulation by millimolar Ca^{2+} or Mg^{2+} (Shi et al., 2002; Xia et al., 2002), protons (Avdonin et al., 2003), Heam-binding (Tang et al., 2003), phosphorylation (Schubert and Nelson, 2001), and oxidation (Tang et al., 2001, 2004).

Although considerable progress has been made in identifying functional elements within the BK channel tail, many features of the structure and function of this very large domain remain unknown. Even where important regions have been characterized, it is often unclear how they interact with each other or the transmembrane core to influence channel activation. An important aspect of the mechanisms by which tail domain elements influence function must be their eventual coupling to channel opening, a linkage that potentially involves multiple protein domains and interactions, including effects on voltage- or Ca^{2+}-dependent gating. Thus, it is likely that the tail domain contains not only regulatory elements that interact directly with signaling molecules, but also regions that are critical for coupling the action of these regulatory elements to the channel gate.

Two RCK (regulator of K^+ conductance) homology domains (RCK1 and RCK2) have been identified within the NH_2-terminal half of the BK channel tail, encompassing several functionally important regions

Correspondence to Frank T. Horrigan: horrigan@mail.med.upenn.edu

Abbreviation used in this paper: WT, wild type.

J. Gen. Physiol. © The Rockefeller University Press • 0022-1295/2005/02/213/24 $8.00
Volume 125 February 2005 213–236
http://www.jgp.org/cgi/doi/10.1085/jgp.200409149

(Jiang et al., 2002; Qian et al., 2002; Tang et al., 2004). The crystal structure of RCK domains are known for several prokaryotic proteins, including the Ca^{2+}-dependent MthK channel (Jiang et al., 2001, 2002), providing a potential model of BK channel structure and function. By analogy with MthK, conformational changes in the BK channel RCK domains are proposed to be coupled to the pore through the S6–RCK1 linker (Jiang et al., 2002). Effects of linker modification on BK channel gating appear consistent with this hypothesis (Niu et al., 2004). However, the RCK domains of BK and MthK channels share <20% sequence identity, suggesting that their structures are not identical and that important differences may exist regarding interactions that occur within the RCK domain and with the rest of the channel protein. For example, a low-affinity Mg^{2+}/Ca^{2+} binding site has been identified in the RCK1 domain that is not present in MthK (Shi et al., 2002; Xia et al., 2002). In addition, Mg^{2+}-dependent activation of BK channels is inhibited by mutations in the S4 and S4–S5 linker, suggesting that interactions exist between the RCK1 domain and voltage sensor, whereas MThK is a two transmembrane channel that has no voltage sensor (Hu et al., 2003).

In the present study, we probed the function of the tail domain by studying changes in BK channel gating produced by various cysteine-modifying reagents (MTSES, MTSET, and NEM) applied to the intracellular side of the channel. Of the 30 cysteine residues present in the mSlo1 BK channel α-subunit, only 3 are in the core domain, and these are located in extracellular regions of the NH_2 terminus, S1–S2 linker, and pore loop. The majority of cysteines (24) are scattered throughout the tail domain and three more are located in the intracellular S0–S1 linker. Cysteine modification by thiol-specific MTS reagents or oxidation has been shown to inhibit BK channel activity (DiChiara and Reinhart, 1997; Tang et al., 2001, 2004; Erxleben et al., 2002). However, the functional changes and cysteines that underlie these changes have been only partially characterized.

Here, we determine the effects of cysteine modification on steady-state and kinetic properties of I_K over a wide range of conditions to determine the impact of modification on voltage- and Ca^{2+}-dependent gating as well as the relative stability of the closed and open conformation. BK channel gating is well described in terms of allosteric mechanisms where the closed–open conformational change does not require Ca^{2+} binding or voltage sensor activation but is promoted by either (Cox et al., 1997a; Horrigan and Aldrich, 1999, 2002; Horrigan et al., 1999; Rothberg and Magleby, 1999, 2000; Cui and Aldrich, 2000). By measuring steady-state activation under conditions that include 0 Ca^{2+} and extreme negative voltages, we can isolate effects on the closed–open transition from those on Ca^{2+}- or voltage-dependent gating mechanisms. Moreover, we can distinguish whether perturbations to Ca^{2+}- or voltage-dependent gating reflect changes in the activation of Ca^{2+} or voltage sensors or a change in the coupling of these sensors to channel opening (Horrigan and Aldrich, 2002).

By characterizing in detail the changes in BK channel gating produced by cysteine modification, we seek not only to identify important regions of the tail domain but also to understand the mechanisms by which these regions influence channel function. C911 has been identified previously in hSlo1 as a key cysteine whose modification is largely responsible for inhibitory effects of cysteine oxidation or MTSEA on BK channel activation (Tang et al., 2004). Modification of C911 is thought to inhibit Ca^{2+} binding to the nearby Ca^{2+}-bowl domain (Schreiber and Salkoff, 1997). However, the effects on channel gating of cysteine-modifying reagents in our experiments differ from those described by Tang et al. (2004), and involve additional sites of action. Thus, we find that modification of C615 by MTSET also reduces apparent Ca^{2+} affinity, suggesting that the Heam-binding site, which includes C615, may influence Ca^{2+} binding. In addition, we find that modification of C430 in the RCK1 domain alters the relative stability of closed and open conformations as well as the coupling of both voltage sensor activation and Ca^{2+} binding to channel opening. The impact of C430 is particularly interesting because it lies in a region of the RCK domain that is not present in MthK. The effects on gating of C430 modification, or deletion of a region including C430, are discussed in light of known features of RCK structure and the recent proposal that the BK channel RCK domain exhibits spring-like mechanical properties (Niu et al., 2004).

MATERIALS AND METHODS

Mutagenesis and Channel Expression

Experiments were performed with the mbr5 clone of the mouse homologue of the Slo1 gene (*mSlo1*) (Butler et al., 1993) provided by L. Salkoff (Washington University, St. Louis, MO) in a BlueScript vector (Stratagene), or human homologue hSlo1 (hbr1) (Tseng-Crank et al., 1994) provided by T. Hoshi (University of Pennsylvania, Philadelphia, PA) in pCI-neo vector (Promega). hSlo1 point mutants (C348A, C422A, C430A, C615S, C628S, C630S, and C911A) and C(1–13)A, C(18–29)A, and C(1–13)AC(18–29)A constructs were also provided by T. Hoshi (Tang et al., 2001; Avdonin et al., 2003). For constructs containing multiple C to A mutations, the numbers in parentheses refer to sequentially numbered cysteines where the actual position in hSlo1 or mSlo1 are 14, 53, 54, 56, 141, 277, 348, 422, 430, 485, 498, 554, 557, 612, 615, 628, 630, 695, 722, 797, 800, 820, 911, 975, 995, 1001, 1011, 1028, and 1051. The hSlo1-ΔD construct in which eight amino acids were deleted (428–435) was prepared by overlap extension PCR, subcloned into full-length hSlo1-pCI-neo, and verified by sequencing. cRNA for mSlo1 was synthesized

from BamH1-linearized cDNA using T3 polymerase and for hSlo1 and hSlo1 mutants from Not1-linearized cDNA using T7 polymerase. *Xenopus* oocytes were injected with ~0.5–5 ng of cRNA 4–20 d before recording and maintained at room temperature.

Electrophysiology

Currents were recorded using the patch clamp technique in the inside out configuration (Hamill et al., 1981). Upon excision, patches were washed with at least 20× volumes of internal solution. K^+ currents were recorded with internal solutions containing (in mM) 110 $KMeSO_3$ and 20 HEPES and an external (pipette) solution containing 100 $KMeSO_3$, 10 KCl, 2 $MgCl_2$, 20 HEPES. Internal solutions contained 40 μM (+)-18-crown-6-tetracarboxylic acid to chelate contaminant Ba^{2+} (Diaz et al., 1996; Neyton, 1996; Cox et al., 1997b). "0 Ca^{2+}" solutions contained 2 mM EGTA reducing free Ca^{2+} to an estimated 0.8 nM based on the presence of ~10 μM contaminant Ca^{2+} (Cox et al., 1997b). Ca^{2+} solutions were buffered with 5 mM HEDTA, and free Ca^{2+} was measured with a Ca^{2+} electrode (Orion Research Inc.). Nominal [Ca^{2+}] reported as 1, 5, 10, 20, and 70 μM correspond to measured concentrations of 1.3, 4.4, 9.9, 17, and 66 μM, respectively. Ca^{2+} was added as $CaCl_2$, and [Cl^-] was adjusted to 10 mM with HCl. The pH of all solutions was 7.2. Solutions were prepared and experiments performed at room temperature (22–24°C).

Electrodes were pulled from thick-walled 1010 glass (World Precision Instruments), coated with wax (KERR sticky wax) and fire polished before use. Pipette access resistance measured in the bath solution (0.8–1.5 MΩ) was used as an estimate of series resistance (R_s) to correct the voltage at which I_K was recorded. The corrected voltage was used in determining membrane conductance (G_K) from tail current measurements and in plotting the voltage dependence of G_K. Series resistance error was <15 mV for all data presented.

Data were acquired with an Axopatch 200B amplifier (Axon Instruments) set in patch mode with the amplifier's internal 4-pole Bessel filter set at 100 kHz. Currents were subsequently filtered by an 8-pole Bessel filter (Frequency Devices Inc.) at 20 kHz and sampled at 100 kHz with an 18 bit A/D converter (Instrutech ITC-18). A P/4 protocol was used for leak subtraction (Armstrong and Bezanilla, 1974) with a holding potential of −80 mV. A Macintosh-based computer system was used in combination with Pulse Control acquisition software (Herrington and Bookman, 1995) and Igor Pro for graphing and data analysis (WaveMetrics Inc.). A Levenberg-Marquardt algorithm was used to perform nonlinear least-squared fits.

Under conditions where the open probability (P_O) is small ($<10^{-3}$), unitary currents were observed in patches containing hundreds of channels, and NP_O was determined from steady-state recordings of 1–60 s duration that were digitally filtered at 5 kHz. NP_O was determined from all-points amplitude histograms by measuring the fraction of time spent (P_k) at each open level (k) using a half-amplitude criteria and summing their contributions $NP_o = \sum kP_k$. P_o was determined by combining NP_O measurements with an estimate of $N = G_{Kmax}/g_K$, where G_{Kmax} was determined by fitting a Boltzmann function ($G_K = G_{Kmax}[1 + \exp(-ze(V - V_h)/kT)]^{-1}$) to the macroscopic G_K–V relation in the same patch, and g_K is the single channel conductance.

Patch to patch variations in the half-activation voltage of G_K–V relations are observed for *mSlo1* (Horrigan et al., 1999) and *hSlo1* (Stefani et al., 1997), possibly due to differences in the redox state of channels (DiChiara and Reinhart, 1997; Tang et al., 2001). Such variation causes broadening in averaged voltage-dependent relationships relative to individual experiments. To compensate for this effect, V_h was determined for each patch and compared with the mean for all experiments ($<V_h>$) at the same [Ca^{2+}]. G_K–V relations from individual experiments were then shifted along the voltage axis to $<V_h>$ before averaging. This procedure yields average relations that more accurately represent the shape of individual G_K–Vs. To determine average G_K–V relations for channels modified by MTSES, MTSET, or NEM, the G_K–V shift produced by steady-state modification $\Delta V_h = V_h$ (modified) − V_h (control) was determined from individual experiments, and the modified G_K–Vs in each [Ca^{2+}] were shifted to a mean V_h ($<V_h(\text{modified})> = <V_{h\,control}> + <\Delta V_h>$) before averaging. In this way, the relative position of mean G_K–V relations and V_h–[Ca^{2+}] relations before and after modification accurately reflect the mean G–V shift ($<\Delta V_h>$) rather than patch to patch differences in V_h for control and modified G_K–Vs that were averaged from different experiments.

Reagents

MTSET ([2-(trimethylammonium)ethyl] methanethiosulfonate bromide) and MTSES (sodium (2-sulfanatoethyl) methanethiosulfonate) were obtained from Toronto Research Chemicals, dissolved in water at 100 mM and 1 M, respectively, and stored at −20°C. During experiments, aliquots were thawed and stored on ice for not longer than 30 min before diluting 1,000-fold into the appropriate internal solution just before application. NEM (*N*-ethyl maleimide; Sigma-Aldrich) was prepared at 250 mM in internal solutions containing different Ca^{2+} and stored at 4°C before diluting into the same internal solution at 20 mM immediately before use. Solution exchange and reagent applications were done manually within ~5 s by exchanging the bath solution (200 μl) with 5–20 volumes of internal solution.

RESULTS

Effects of Cysteine-modifying Reagents on mSlo1 Channel Function

To study the effects on BK channel gating of modifying cysteine residues, membrane patches expressing mSlo1 channels were excised from *Xenopus* oocytes in the inside-out configuration and the thiol-reactive reagents, MTSES, MTSET, or NEM, were applied by exchanging the bath solution. MTSES(−) and MTSET(+) are charged and presumably modify only cysteines accessible from the intracellular solution, whereas NEM is membrane permeable and may modify additional sites. Spontaneous changes in BK channel gating, including a shift in the G_K–V relation to more positive voltages, are often observed following patch excision and may reflect oxidation of cysteine and/or methionine residues (DiChiara and Reinhart, 1997; Tang et al., 2001). Therefore, we typically waited ~30 min following patch excision to allow the G_K–V relation to stabilize, before acquiring control records and applying cysteine-modifying reagents. While this procedure may allow some cysteines to become oxidized, it assures that effects of cysteine-modifying reagents were studied in the virtual absence of spontaneous changes in gating.

During reagent application, the membrane was held at −80 mV, and macroscopic potassium currents (I_K) were evoked by brief 25-ms test pulses every 10 s to a potential near the half-activation voltage (V_h). Fig. 1

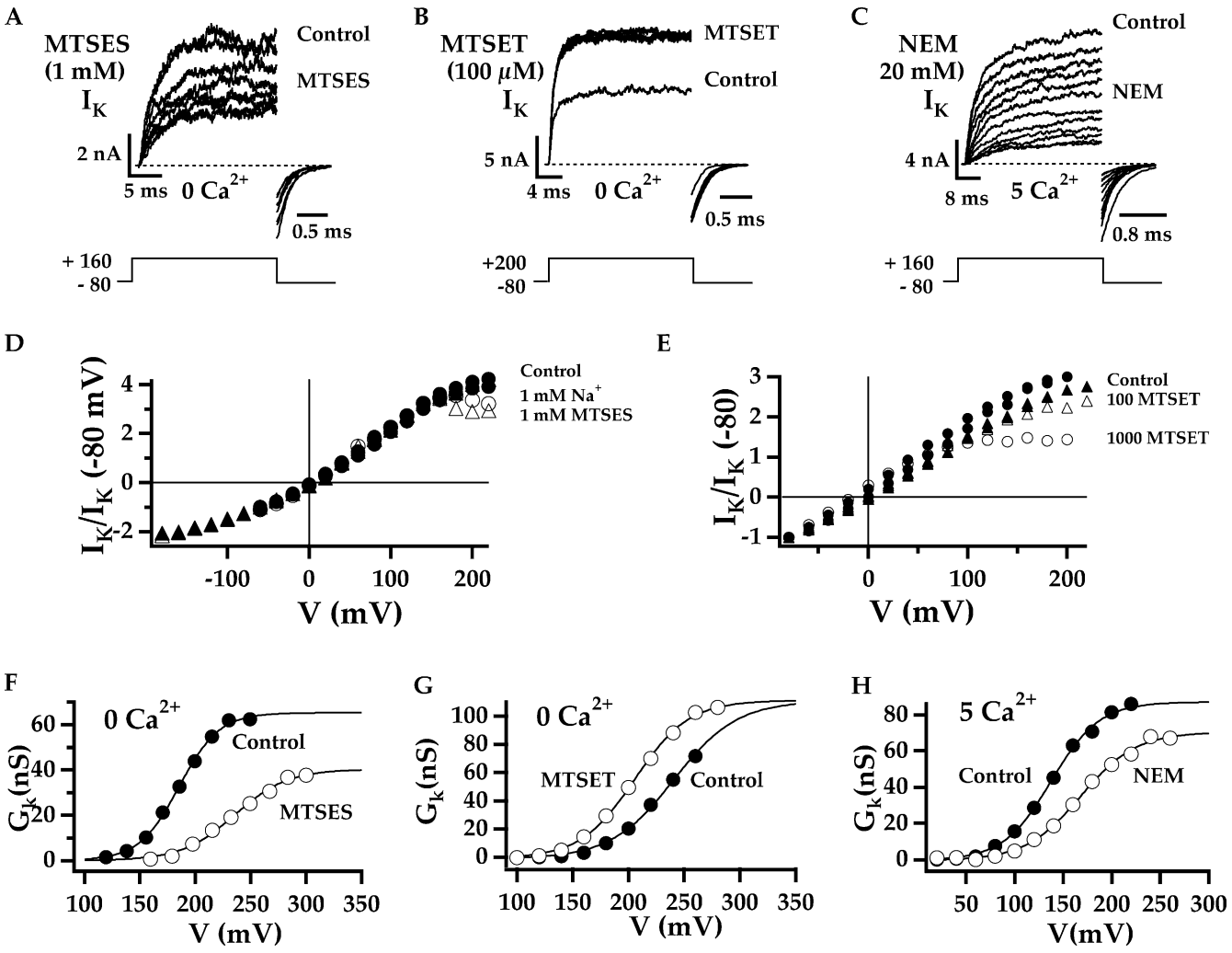

FIGURE 1. Modification and block of mSlo1 channels by MTSES, MTSET, and NEM. (A–C) I_K evoked by 25-ms pulses to the indicated voltage before (control) and during treatment with the indicated cysteine-modifying reagent. MTSES in 0 Ca^{2+} or NEM in 5 μM Ca^{2+} cause a slow decrease in both steady-state and tail I_K, whereas MTSET in 0 Ca^{2+} causes a rapid increase. Test pulses were delivered every 10 s from a holding potential of −80 mV, and reagent was applied by exchanging the bath solution. I_K during the pulse and tail currents immediately following the pulse are plotted on different time scales (see scale bars). I_K was plotted for each test pulse in the case of MTSET and MTSET but was plotted for every third pulse in the case of NEM. (D and E) Instantaneous I_K–V relations in the presence or absence of MTS reagents demonstrate that channels are reversibly blocked at positive voltages. (D) The effect of 1 mM Na-MTSES (Δ) and 1 mM NaCl (O) are similar, suggesting that the Na^+ counter ion is responsible for the blocking effect of MTSES. (E) 1000 μM MTSET (O) blocks I_K by 50% at +200 mV, but a much smaller effect is seen with 100 μM MTSET (Δ). I–Vs were determined by maximally activating channels with a test pulse (V = +200 mV, [Ca^{2+}] = 5 μM) and measuring I_K at different voltages immediately following the test pulse. Controls obtained before reagent application and after washout (filled symbols) were normalized at −80 mV. I–Vs in the presence of reagent were measured after steady-state modification and were normalized to I_K (−80) of the corresponding washout I–V. (F–H) G_K–V relations determined from isochronal tail currents at −80 mV before (control) and after steady-state modification by the indicated reagent, corresponding to the conditions in A–C. Control and modified G–Vs were measured in the same solutions (in the absence of reagent) and are fit by Boltzmann functions. MTSES in 0 Ca^{2+} increases V_h and decreases G_{Kmax} (control: V_h = 210 mV, G_{Kmax} = 71 nS, z = 1.397 *e*; MTSES: V_h = 249 mV, G_{Kmax} = 43 nS, z = 1.059 *e*). A similar effect is observed for NEM in 5 μM Ca^{2+} (control: V_h = 147 mV, G_{Kmax} = 89 nS, z = 1.011 *e*; NEM: V_h = 168 mV, G_{Kmax} = 68 nS, z = 0.907 *e*). However, MTSET in 0 Ca^{2+} produces a decrease in V_h with G_{max} held constant (control: V_h = 237 mV, G_{Kmax} = 105 nS, z = 1.13 *e*; MTSET: V_h = 207 mV, G_{Kmax} = 105 nS, z = 1.048 *e*).

(A–C) shows the effect on I_K of 1 mM MTSES, 100 μM MTSET, and 20 mM NEM, respectively. MTSES, applied in the absence of Ca^{2+}, produced a gradual decrease in both I_K evoked at +160 mV and tail current following the test pulse (Fig. 1 A). An approximate 60% steady-state decrease in current amplitude was observed after 250 s. By contrast, MTSET in 0 Ca^{2+} produced a rapid twofold increase in I_K within the 10-s interval between test pulses (Fig. 1 B). NEM, like MTSES, produced a gradual decrease in I_K, achieving an 80% steady-state reduction in 300 s in the presence of 5 μM Ca^{2+} (Fig. 1 C).

Most effects of MTSES, MTSET, or NEM were not reversed by washout of the reagent and presumably reflect modification of cysteine residues. However, a small increase in outward current was often observed immediately upon washout of MTSES or MTSET. This increase reflects relief of channel block by the MTS reagent or its counter-ion. Instantaneous current–voltage relations obtained in the presence and absence of MTSES (Fig. 1 D) or MTSET (Fig. 1 E) demonstrate this blocking effect. At negative voltages, I_K is unaffected by washout. However, the I–V relation, which is relatively linear in the absence of reagent, rectifies in the presence of MTSES or MTSET such that I_K is reduced increasingly at more positive voltages. This rectification is consistent with rapid voltage-dependent block by a positively charged ion from the intracellular solution. In the case of MTSET(+), the reagent itself may block the channel. In the case of MTSES(−), the counter-ion Na^+ is known to block BK channels (Kehl, 1996; Morales et al., 1996); and 1 mM NaCl reproduces the effect of 1 mM Na-MTSES on the I–V relation (Fig. 1 D).

To minimize the influence of channel block on analysis of cysteine modification, concentrations of MTSET and MTSES were limited to 100 μM and 1 mM, respectively. In addition, the time course of modification and conductance–voltage (G_K–V) relations were determined by measuring tail currents at a voltage (−80 mV) where block is negligible. Finally, reagent was washed out after steady-state modification when possible so that I_K could be compared before and after modification in the absence of reagent. G_K–V relations obtained in this way before and after modification by MTSES (Fig. 1 F), MTSET (Fig. 1 G), and NEM (Fig. 1 H) indicate that changes in I_K amplitude observed in Fig. 1 (A–C) reflect a shift of the G_K–V along the voltage axis and, for MTSES and NEM, a decrease in G_{Kmax} estimated from fits to a Boltzmann function.

Effects of Cysteine Modification are Ca^{2+} Dependent

Because BK channel activation is Ca^{2+} dependent, we examined the effects of applying cysteine-modifying reagents in different $[Ca^{2+}]_i$, from 0 to 70 μM. At each $[Ca^{2+}]_i$, test pulse voltage was less than or equal to V_h such that I_K should change if the G_K–V relation is altered. However, marked differences in the extent to which I_K changed were observed in different $[Ca^{2+}]_i$ (Fig. 2).

In contrast to the I_K decrease produced by MTSES in 0 Ca^{2+} (Fig. 1 A), MTSES in 5 μM Ca^{2+} had almost no effect on tail I_K and produced only a small immediate decrease in outward current, consistent with Na^+ block (Fig. 2 A). Fig. 2 B plots G_K determined from tail current amplitude versus time for experiments in 0 Ca^{2+} and 5 μM Ca^{2+}, similar to those in Fig. 1 A and Fig. 2 A. In 0 Ca^{2+}, G_K was stable before MTSES was applied and then decreased by almost 80% to a steady state within 500 s, with a time course that can be approximated by an exponential function (line, $\tau = 61$ s). In 5 μM Ca^{2+}, G_K decreased by <10% over the same time period. This small slow decrease cannot be distinguished from the spontaneous rundown of G_K that sometimes occurs in the absence of reagent presumably due to channel oxidation. A similar failure of MTSES to alter G_K was observed at all $[Ca^{2+}]_i > 1$ μM (unpublished data).

MTSET and NEM, unlike MTSES, significantly altered G_K in 5 μM Ca^{2+}. 100 μM MTSET increased G_K by 50% with a time course, as in 0 Ca^{2+}, that was too rapid to resolve (Fig. 2 D). 20 mM NEM decreased G_K by >80% with an exponential time course ($\tau = 127$ s; Fig. 2 F). However, conditions were also identified where changes in G_K produced by MTSET or NEM are small. Surprisingly, MTSET did not alter G_K in 1 μM Ca^{2+} (Fig. 2, C and D), although increases were observed in both higher (5 μM) and lower (0) $[Ca^{2+}]_i$ (Fig. 2 D). Conversely, the effect of NEM on G_K in 0 Ca^{2+} (Fig. 2, E and F) or 70 μM Ca^{2+} (Fig. 2 F) was much less than that observed in 5 μM Ca^{2+}.

Cysteine Modification is Not Prevented by Ca^{2+} Binding

The results in Fig. 2 demonstrate that interaction among cysteine-modifying reagents, Ca^{2+}, and BK channel gating is complex. Not only are the effects of MTSES, MTSET, and NEM on G_K Ca^{2+} dependent, but the pattern of Ca^{2+} dependence for each reagent is different. To understand these results, it's important to distinguish between channel modification and the modification effect. Modification refers to the reaction of reagent with the BK channel protein, most likely forming a covalent bond with one or more cysteine residues. The modification effect is the change in channel function produced by cysteine modification. Although a modification effect indicates that cysteines have been modified, the converse is not necessarily true. That is, failure to observe a modification effect does not indicate a lack of cysteine modification if modification has no effect on function or produces complex changes in channel gating that are difficult to detect.

Two mechanisms could account for the failure to observe a modification effect at certain $[Ca^{2+}]_i$ in Fig. 2. First, the accessibility of cysteine residues to reagent might be state dependent such that the rate of modification is influenced by Ca^{2+} binding. That is, modification of key cysteines might be inhibited by the presence or absence of Ca^{2+}. Second, cysteine modification might alter the Ca^{2+} sensitivity of channel gating such that the change in G_K produced by modification at each $[Ca^{2+}]_i$ is different. Experiments shown in Fig. 3 suggest that the latter mechanism accounts for the results in Fig. 2.

To test whether failure to observe a modification effect reflects a failure to modify cysteines, we first ap-

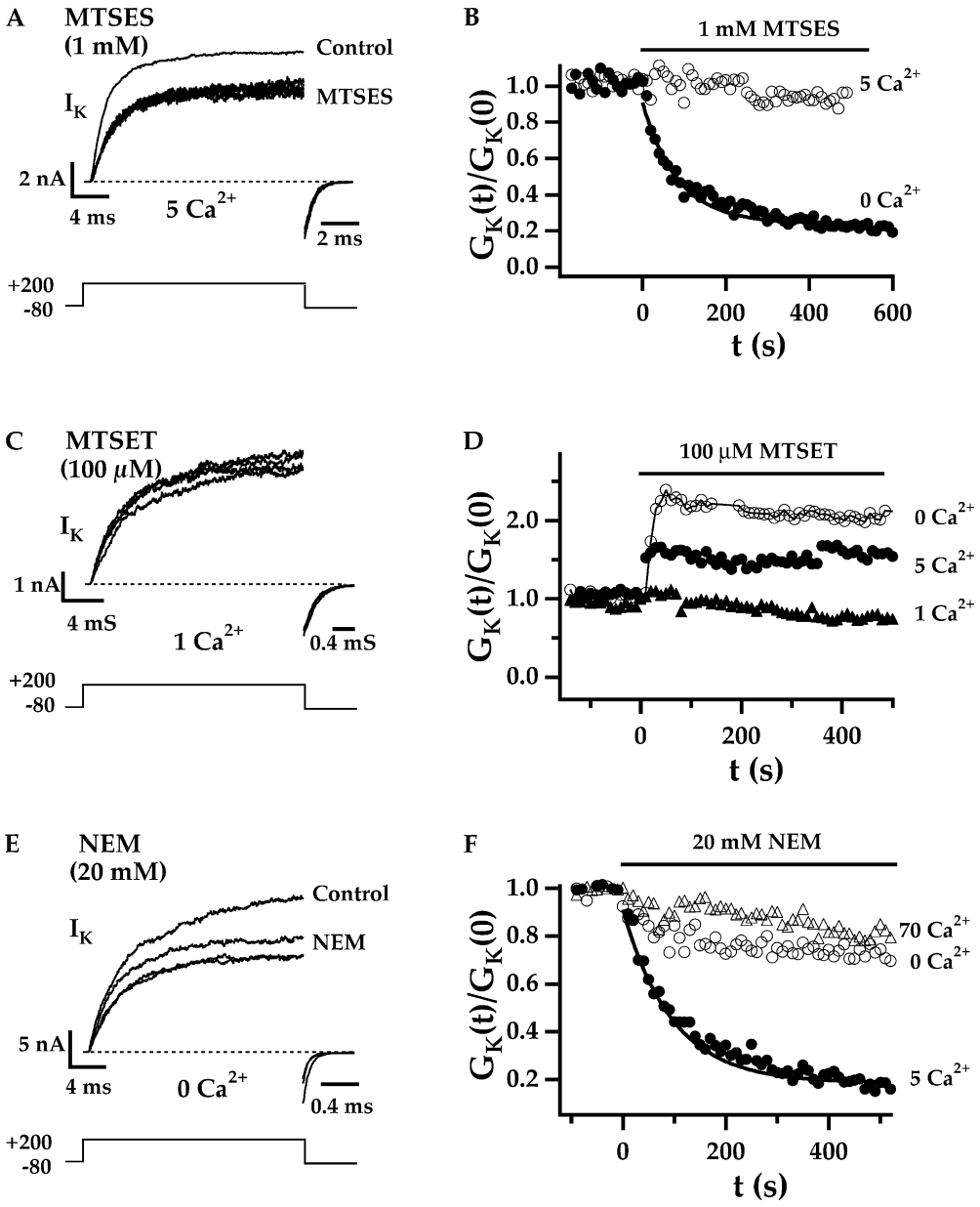

FIGURE 2. The effects of cysteine-modifying reagents on I_K are Ca^{2+} dependent. (A) I_K evoked during test pulses to +200 mV in 5 μM Ca^{2+} is reduced immediately by 1 mM MTSES without altering tail current, consistent with reversible block (see Fig. 1 D) rather than a change in P_o. (B) G_K, determined for each test pulse from tail current amplitude at −80 mV and normalized to $t = 0$, is plotted versus time as 1 mM MTSES is applied either in 5 μM Ca^{2+} (V_{test} = +160 mV) or 0 Ca^{2+} (V_{test} = +200 mV). The time course of G_K decay in 0 Ca^{2+} is fit by an exponential function (line, τ = 61 s). (C) MTSET has little effect on I_K evoked by +200-mV pulses in 1 μM Ca^{2+}. (D) G_K in 0 Ca^{2+} (V_{test} = +200 mV) or 5 μM Ca^{2+} (V_{test} = +140 mV) is increased rapidly by 100 μM MTSET, but no similar response is observed in 1 μM Ca^{2+} (V_{test} = +180 mV). (E) NEM reduces both outward and tail I_K evoked by +200-mV test pulses in 0 Ca^{2+}. (F) G_K is slowly reduced by 20 mM NEM in 0 Ca^{2+} (V_{test} = +200 mV), 5 μM Ca^{2+} (V_{test} = +140 mV), or 70 μM Ca^{2+} (V_{test} = +40 mV). However, the decrease is greatest in 5 μM Ca^{2+}, where the time course of G_K decay is fit by an exponential function (line, τ = 127 s).

plied reagent at $[Ca^{2+}]_i$ where no modification effect is observed and then assayed for modification by either changing $[Ca^{2+}]_i$ (Fig. 3, A and B) or applying a second reagent (Fig. 3, C and D).

Fig. 3 A plots G–V relations in 20 and 70 μM Ca^{2+} before and after application of NEM. The corresponding sequence of solution changes and V_h measurements are indicated in Fig. 3 B. G–Vs were initially measured in 20 and 70 μM Ca^{2+}, and then 20 mM NEM was applied for 300 s in the presence of 70 μM Ca^{2+}, producing no change in V_h (Fig. 3 B) or G_K (Fig. 2 F). G–Vs obtained in 70 μM Ca^{2+} before application of NEM and after washout are indistinguishable (Fig. 3 A). However, the G–V in 20 μM Ca^{2+} measured after washout of NEM was shifted by −16 mV relative to the control, similar to a −22 ± 5 mV shift (mean ± SEM) observed when NEM was applied in the presence of 20 μM Ca^{2+}. Thus NEM in 70 μM Ca^{2+} does modify cysteines and alter channel gating despite failure to alter steady-state activation in 70 μM Ca^{2+}.

Fig. 3 (C and D) plots G_K in 5 μM Ca^{2+} as MTSES is applied for ~200 s before applying NEM or MTSET, respectively. When applied individually in 5 μM Ca^{2+}, MTSES has no effect on G_K, whereas NEM decreases G_K by >80% (Fig. 2 F; Fig. 3 C, line) and MTSET increases G_K by ~50% (Fig. 2 D; Fig. 3 D, line). However, MTSES pretreatment prevents the effects of NEM and MTSET (Fig. 3, C and D, symbols). This result indicates that cysteines are modified by MTSES in 5 μM Ca^{2+} despite the failure to alter G_K. Moreover, MTSES must modify the cysteines

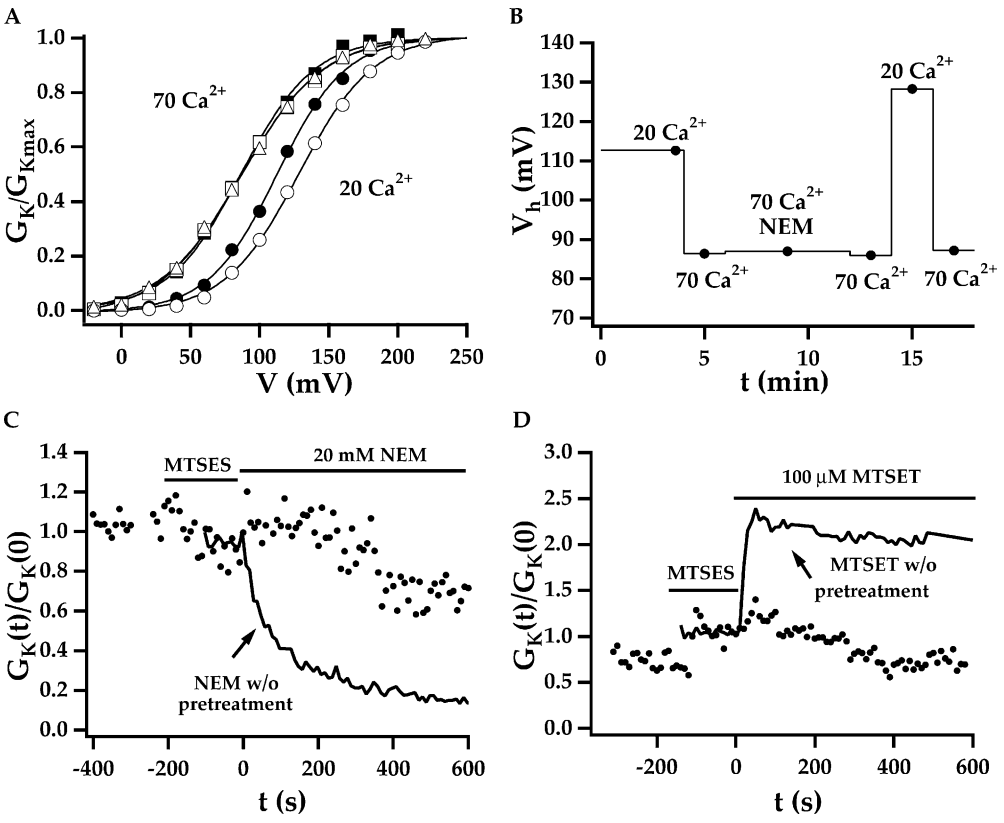

FIGURE 3. Cysteine modification is not prevented by changing $[Ca^{2+}]_i$. (A) Normalized G_K–V relations from a single patch in 20 and 70 μM Ca^{2+} before (filled symbols) and after (open symbols) treatment with 20 mM NEM for 300 s in 70 μM Ca^{2+} are fit by Boltzmann functions. (B) The time sequence of solution changes and V_h measurements for the experiment in A. Controls were measured in 20 and 70 μM Ca^{2+}, and then NEM was applied and washed out in the presence of 70 μM Ca^{2+}, producing no change in V_h. However, subsequent measurement of V_h in 20 μM Ca^{2+} was shifted by −16 mV relative to the control, indicating that channels were modified by NEM in 70 μM Ca^{2+}. (C and D) G_K measured from test pulse tail currents in 5 μM Ca^{2+} (V_{test} = +160 mV) (•) are plotted versus time as patches are pretreated with 1 mM MTSES for the indicated period before applying 20 mM NEM (C) or 100 μM MTSET (D). MTSES pretreatment prevents the effects of NEM or MTSET, indicating that channels were modified by MTSES in 5 μM Ca^{2+} and that MTSES modifies the same cysteines as MTSET and NEM. The responses to NEM or MTSET without MTSES pretreatment are indicated by solid lines taken from Fig. 2, B and D, respectively.

that underlie the modification effects of MTSET and NEM. This conclusion is supported by observations that MTSET pretreatment prevents the modification effects of NEM and MTSES (unpublished data). Thus, all three reagents appear to modify the same cysteine residues.

Effects of Cysteine Modification on I_K Kinetics

Changes in steady-state activation produced by cysteine modification are accompanied by changes in I_K kinetics (Fig. 4). Comparison of normalized currents evoked by voltage pulses before and after MTSES treatment in 0 Ca^{2+} (Fig. 4 A) shows that modification slows I_K activation at +240 mV 2.4-fold but has no effect on tail current decay at −80 mV. This is also evident in Fig. 4 B, which plots the time constants of I_K relaxation ($\tau(I_K)$) at different voltages in 0, 5, and 70 μM Ca^{2+} before and after steady-state modification. In 0 Ca^{2+}, $\tau(I_K)$ is increased at $V \geq +200$ mV but is unchanged from +240 to +180 mV. That $\tau(I_K)$ increases only at the most positive voltages suggests that cysteine modification slows the rate-limiting forward transitions from closed to open (activation) without altering the reverse transition (deactivation), consistent with a decrease in open probability and shift of the G–V to more positive voltages in 0 Ca^{2+} (Fig. 1 F). Likewise, $\tau(I_K)$ is not altered in 70 μM Ca^{2+} (Fig. 4 B), consistent with the lack of a G–V shift in high $[Ca^{2+}]$. However, in 5 μM Ca^{2+}, activation is slowed (Fig. 4, A and B), although I_K amplitude is unchanged (Fig. 2 B; Fig. 3, C and D). This result provides additional evidence that channels are modified even when steady-state activation is unchanged, and suggests that MTSES does not act merely to alter the rate-limiting transition.

MTSET slows I_K deactivation without affecting activation (Fig. 4, C and D), an effect opposite to that of MTSES. The time course of I_K evoked during a pulse to +240 mV in 0 Ca^{2+} is unchanged by MTSET, but the tail current decay at −80 mV is slowed (Fig. 4 C). $\tau(I_K)$–V relationships in 0, 5, or 70 μM Ca^{2+} (Fig. 4 D) exhibit similar responses to MTSET, increasing at voltages more negative than peak $\tau(I_K)$ and unchanged at the most positive voltages. A slowing of deactivation is consistent with the increase in steady-state activation observed at these $[Ca^{2+}]$. Likewise, in 1 μM Ca^{2+}, no change in either I_K kinetics (Fig. 4 C) or amplitude (Fig. 2 D) is observed.

Effects of NEM on the $\tau(I_K)$–V relation were not examined. However, the response to test pulses in 0, 10,

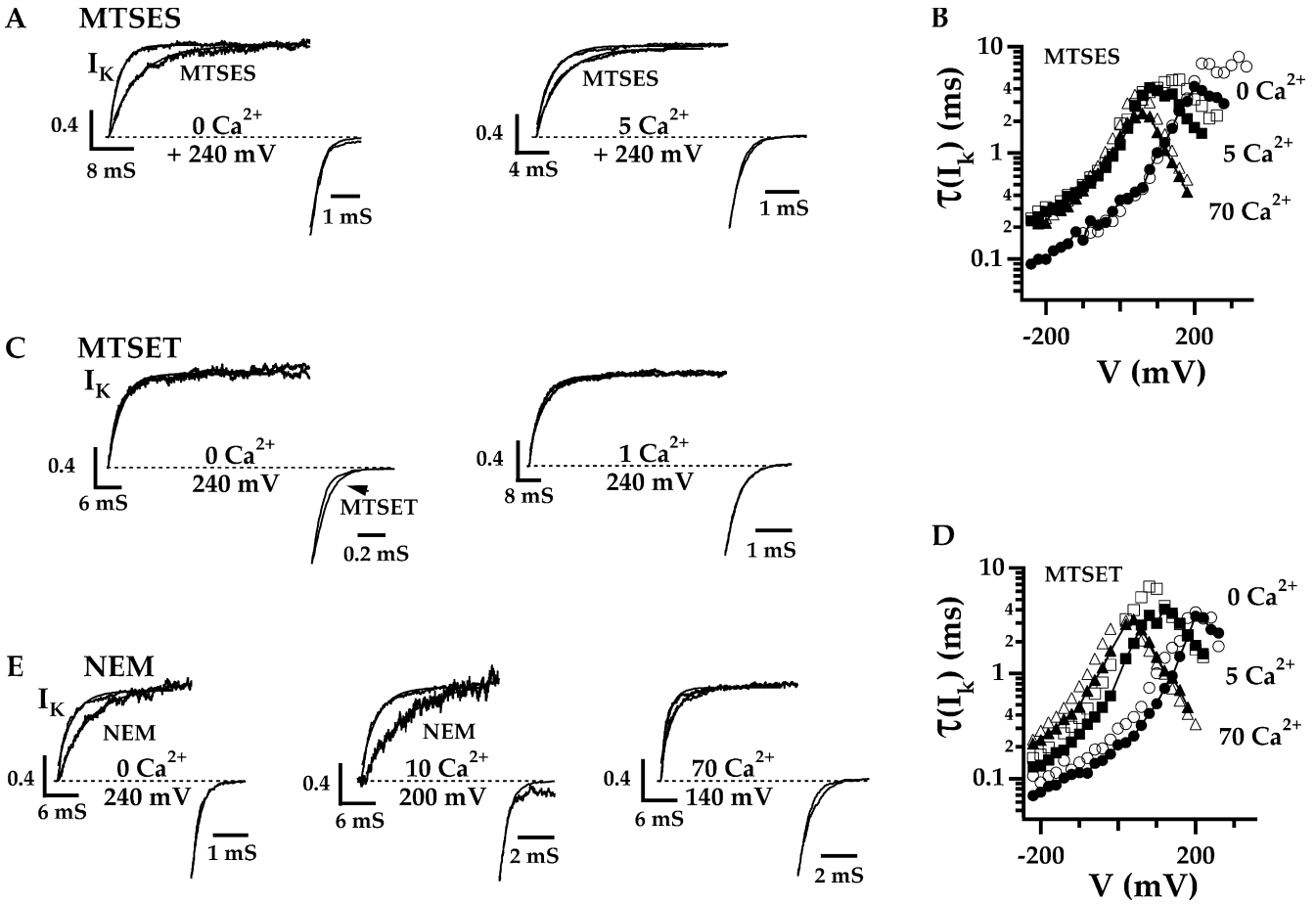

FIGURE 4. Effects of cysteine modification on I_K kinetics. (A, C, and E) Normalized I_K evoked by 25-ms pulses to the indicated voltages from a holding potential of −80 mV are compared before and after steady-state modification by MTSES (A), MTSET (C), or NEM (E) at different $[Ca^{2+}]$. Traces were normalized to steady-state I_K determined from exponential fits (lines). Tail currents are plotted on an expanded scale. (B and D) Time constants of I_K relaxation ($\tau(I_K)$) are plotted versus voltage for 0, 5, and 70 μM Ca^{2+} before (open symbols) and after steady-state modification (closed symbols) by MTSES (B) or MTSET (D). The three pairs of curves in each graph are from separate patches, each corresponding to a different $[Ca^{2+}]$. $\tau(I_K)$ was determined at the most positive voltages by fitting I_K activation with an exponential function as in A, C, and E. At more negative voltages, channels were activated by a 25-ms test pulse, and $\tau(I_K)$ was determined from the tail current decay at different voltages.

and 70 μM Ca^{2+} (Fig. 4 E) reveals a slowing of I_K activation with little effect on tail current decay, similar to the effect of MTSES and consistent with the decrease in steady-state activation produced by NEM (Fig. 2 F).

Cysteine Modification Alters the Ca^{2+} Dependence of Steady-state Activation

The above results indicate that cysteines are modified even at $[Ca^{2+}]_i$ where no change in steady-state activation is evident. Therefore the apparent Ca^{2+} sensitivity of MTSES, MTSET, and NEM action (Figs. 1 and 2) must reflect effects of cysteine modification on the Ca^{2+} dependence of channel gating rather than effects of Ca^{2+} binding on cysteine accessibility. To further characterize changes in Ca^{2+}-dependent gating, we determined G_K–V relations at many $[Ca^{2+}]_i$ before and after steady-state modification (Figs. 5 and 6). In these experiments, control data were recorded at various $[Ca^{2+}]_i$, and then cysteine-modifying reagents were applied at $[Ca^{2+}]_i$ where the extent of modification could be monitored, as in Fig. 1, until a steady-state current amplitude was attained. Subsequently, the reagent was washed out and G–Vs for the modified channels were determined in different $[Ca^{2+}]_i$.

Fig. 5 A shows a series of control G_K–V relations measured at different $[Ca^{2+}]_i$ from a single patch. The data are fit by Boltzmann functions (solid lines), characterized in terms of V_H, G_{Kmax}, and apparent charge (z). Increasing $[Ca^{2+}]_i$ from 0 to 70 μM shifts the G–V to more negative voltages, decreasing V_h by 180 mV, similar to previous reports (Cui et al., 1997; Horrigan and Aldrich, 2002). However, in contrast to previous studies, V_h is ∼60 mV more positive at all $[Ca^{2+}]_i$, and the estimated G_{Kmax} decreases at low Ca^{2+} (<5 μM), rather

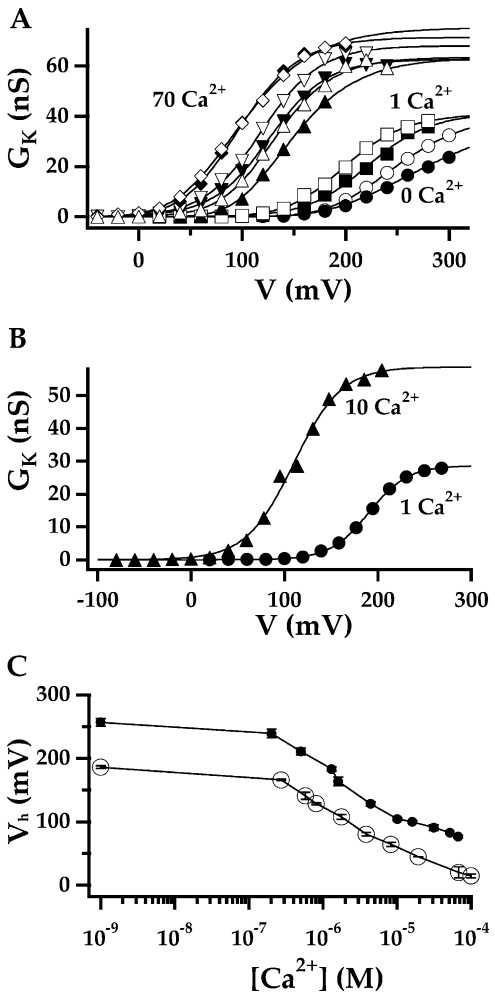

FIGURE 5. The Ca^{2+} dependence of steady-state activation. (A) Control G_K–V relations for mSlo1 from a single patch are fit by Boltzmann functions (lines) illustrating changes in both V_h and estimated G_{Kmax} with $[Ca^{2+}]$ (in μM: 0 [●], 0.3 [○], 0.6 [■], 1.3 [□], 4.4 [▲], 10 [△], 17 [▼], 31 [▽], 51 [◆], 66 [◇]). For $[Ca^{2+}] < 1$ μM, G–Vs were fit using G_{Kmax} determined from the 1 μM Ca^{2+} fit. (B) G_K–V relations from another patch confirm that G_K appears to saturate in 1 μM Ca^{2+} at a lower G_{Kmax} than in 10 μM Ca^{2+}. (C) V_h–$[Ca^{2+}]$ relation from the present study (●) (mean ± SEM) is similar in shape to that from a previous study of mSlo1 (O) (Horrigan and Aldrich, 2002) but shifted to more positive voltages. Control measurements in the present study were determined ~30 min following patch excision to allow spontaneous changes in activation, including increases in V_h, to stabilize before testing effects of cysteine-modifying reagents.

than remains constant. These two differences may be related and probably reflect that membrane patches in the current study were excised for an extended period (~30 min) before G–Vs were recorded.

That G_{Kmax} appears to decrease in low Ca^{2+} is relevant to our analysis because estimation of V_h is dependent on the value of G_{Kmax} used to fit the G_K–V relation. If G_{Kmax} is not constant, the V_h–$[Ca^{2+}]$ relation will be influenced by our ability to estimate G_{Kmax} at each $[Ca^{2+}]$. In high $[Ca^{2+}]$ (>5 μM), G_{Kmax} was usually measured directly from the saturation of G_K at positive voltages. In 1–5 μM Ca^{2+}, examples exist where G_K was observed to saturate at voltages approaching +300 mV (e.g., Fig. 5 B). However, G_{Kmax} at these $[Ca^{2+}]$ was more typically estimated by fitting a nearly saturating G–V and allowing all parameters to vary freely as in Fig. 5 A. In this way, G_{Kmax} in 1 μM was estimated to be 66 ± 12% (mean ± SEM) of that in 70 μM Ca^{2+}. For $[Ca^{2+}] \leq 1$ μM, G_{Kmax} could not be reliably estimated and was therefore approximated by the value determined in 1 μM Ca^{2+} (e.g., Fig. 5 A). G_K–V relations fit in this way from different experiments were normalized to G_{Kmax} and averaged to illustrate the effect of Ca^{2+} on V_h (Fig. 6 A). As in previous studies, the normalized G–V shifts along the voltage axis in response to Ca^{2+} with little change in shape. The mean V_h–$[Ca^{2+}]$ relation obtained from these data (filled symbols, Fig. 5 C) is also similar in shape to that obtained from a previous study (open symbols) (Horrigan and Aldrich, 2002) but is shifted to more positive voltages.

The effects of cysteine-modifying reagents on the Ca^{2+} dependence of steady-state activation are shown in Fig. 6. Normalized G–V relations (mean ± SEM) obtained following modification by MTSES (Fig. 6 B), MTSET (Fig. 6 C), or NEM (Fig. 6 D) are similar in shape to the control (Fig. 6 A). The apparent charge (z) determined from Boltzmann fits to these data differ only at $Ca^{2+} < 1$ μM (Fig. 6 E). However, comparison of V_h–$[Ca^{2+}]$ relations for control and modified channels indicate that each reagent has a distinct effect on the Ca^{2+} dependence of steady-state activation (Fig. 6, E–G). MTSES increases V_h at low Ca^{2+} (≤1 μM) but not high Ca^{2+} (Fig. 6 E). MTSET fails to alter V_h over a range of $[Ca^{2+}]$ from 0.5 to 2 μM but decreases V_h at both higher and lower $[Ca^{2+}]$ (Fig. 6 E). NEM appears to shift the V_h–$[Ca^{2+}]$ relation along the Ca^{2+} axis such that V_h increases over a wide range of intermediate $[Ca^{2+}]$ but is unchanged in 0 Ca^{2+} or 70 μM Ca^{2+}.

Effects of Cysteine Modification on Steady-state Activation at Extreme Negative Voltages

The complex effects of MTSES, MTSET, and NEM on the V_h–$[Ca^{2+}]$ relation suggest that cysteine modification alters multiple features of BK channel function. Shifts in the G–V relation may be caused by changes in either Ca^{2+}- or voltage-dependent gating or the energetics of channel opening (Cox et al., 1997a; Cui and Aldrich, 2000; Horrigan and Aldrich, 2002). However, changes in any one of these processes cannot account for the different effects on V_h produced by these reagents. To better determine how each aspect of gating is altered by cysteine modification, we examined steady-state activation at extreme negative voltages (Fig. 7).

BK channels can open in a Ca^{2+}-dependent manner at negative voltages where voltage sensors are not activated

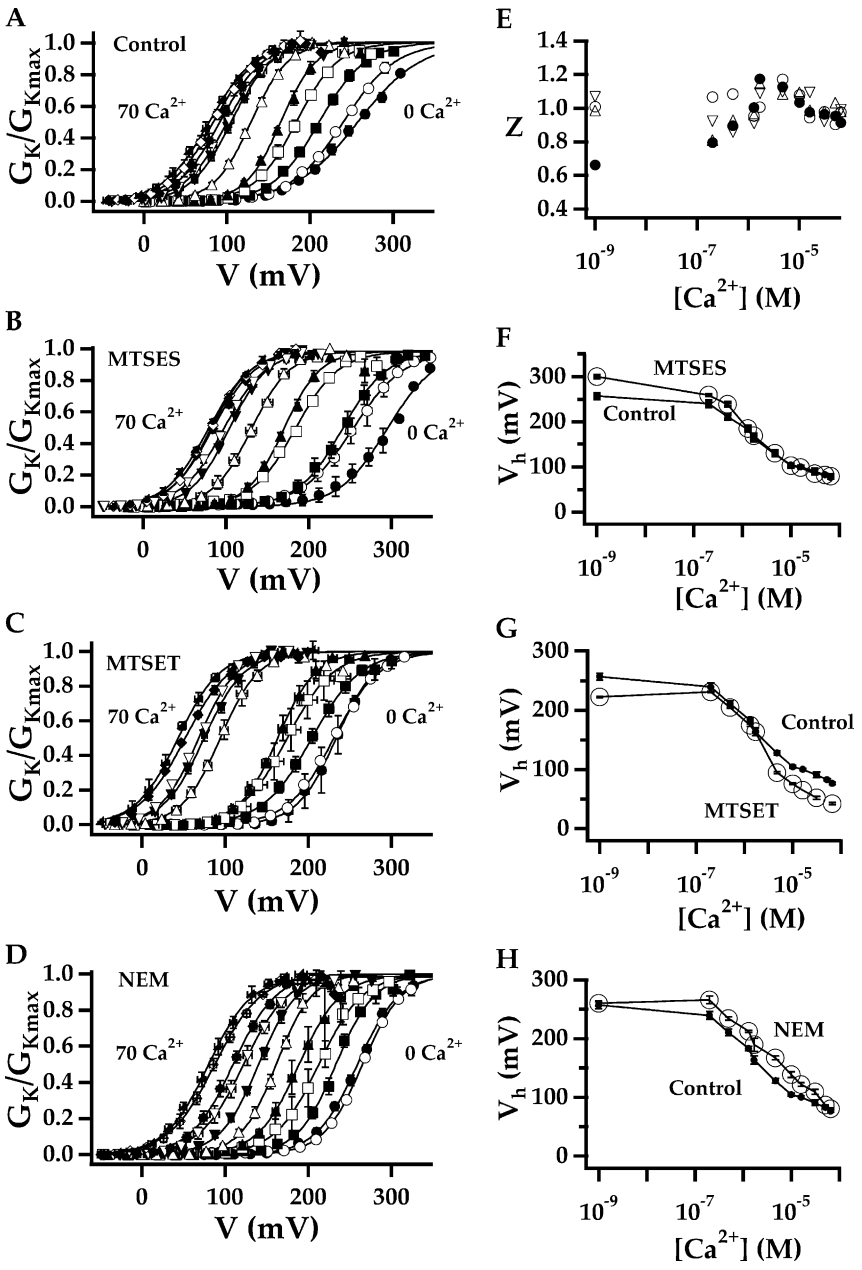

FIGURE 6. Cysteine modification alters the Ca^{2+} dependence of steady-state activation. (A–D) Normalized G_K–V relations (mean ± SEM) in different $[Ca^{2+}]$ (in μM: 0 [●], 0.3 [○], 0.6 [■], 1.3 [□], 2 [▲], 4.4 [△], 10 [▼], 17 [▽], 31 [◆], 51 [◇], 66 [◢]) obtained following steady-state modification by MTSES (B), MTSET (C), or NEM (D) are similar in shape to the control (A) but exhibit different half activation voltages. (E) Apparent charge (z) determined from Boltzmann fits to the mean G–Vs (lines, A–D) are plotted versus $[Ca^{2+}]$ (control [●], MTSES [△], MTSET [▽], NEM [○]). (F–H) V_h–$[Ca^{2+}]$ relations (mean ± SEM) determined from Boltzmann fits to the data in A–D are compared for the control and channels modified by MTSES (F), MTSET (G), and NEM (H), indicating that each reagent has a different effect on the Ca^{2+} dependence of V_H.

(Horrigan et al., 1999). This phenomena is evident as a weakly voltage-dependent plateau in the P_O–V relation at $V < -80$ mV when P_O is plotted on a log scale versus voltage. Control P_O–V relations (mean ± SEM) 0 Ca^{2+} and 70 μM Ca^{2+} are plotted in this way in Fig. 7 A. In 0 Ca^{2+}, P_O at −120 mV is very small ($\sim 10^{-7}$), representing the closed–open equilibrium in the absence of Ca^{2+} binding or voltage sensor activation. However, $P_O(-120)$ increases by almost four orders of magnitude in 70 μM Ca^{2+} (Fig. 7 A), reflecting the strong interaction between Ca^{2+} binding and channel opening. Thus, P_O at extreme negative voltages provides information about Ca^{2+}-dependent gating and the energetics of channel opening in isolation from voltage-dependent gating.

The effects of MTSET on P_O at extreme negative voltages are surprisingly different than those at more positive voltages. P_O–V relations in 0, 5, and 70 μM Ca^{2+} all increase at positive voltages in response to MTSET (Fig. 7 B), corresponding to approximate 40-mV decreases in V_h (Fig. 6 G). However, at −120 mV, P_O decreases in 5 μM Ca^{2+}, increases in 70 μM Ca^{2+}, and is relatively unchanged in 0 Ca^{2+} (Fig. 7, B and C). That the effects of MTSET on P_o at positive and negative voltages are different imply that cysteine modification alters voltage-dependent gating. That MTSET changes $P_O(-120)$ in a Ca^{2+}-dependent manner indicates that Ca^{2+}-dependent gating is also perturbed. However, failure to change $P_O(-120)$ in 0 Ca^{2+} sug-

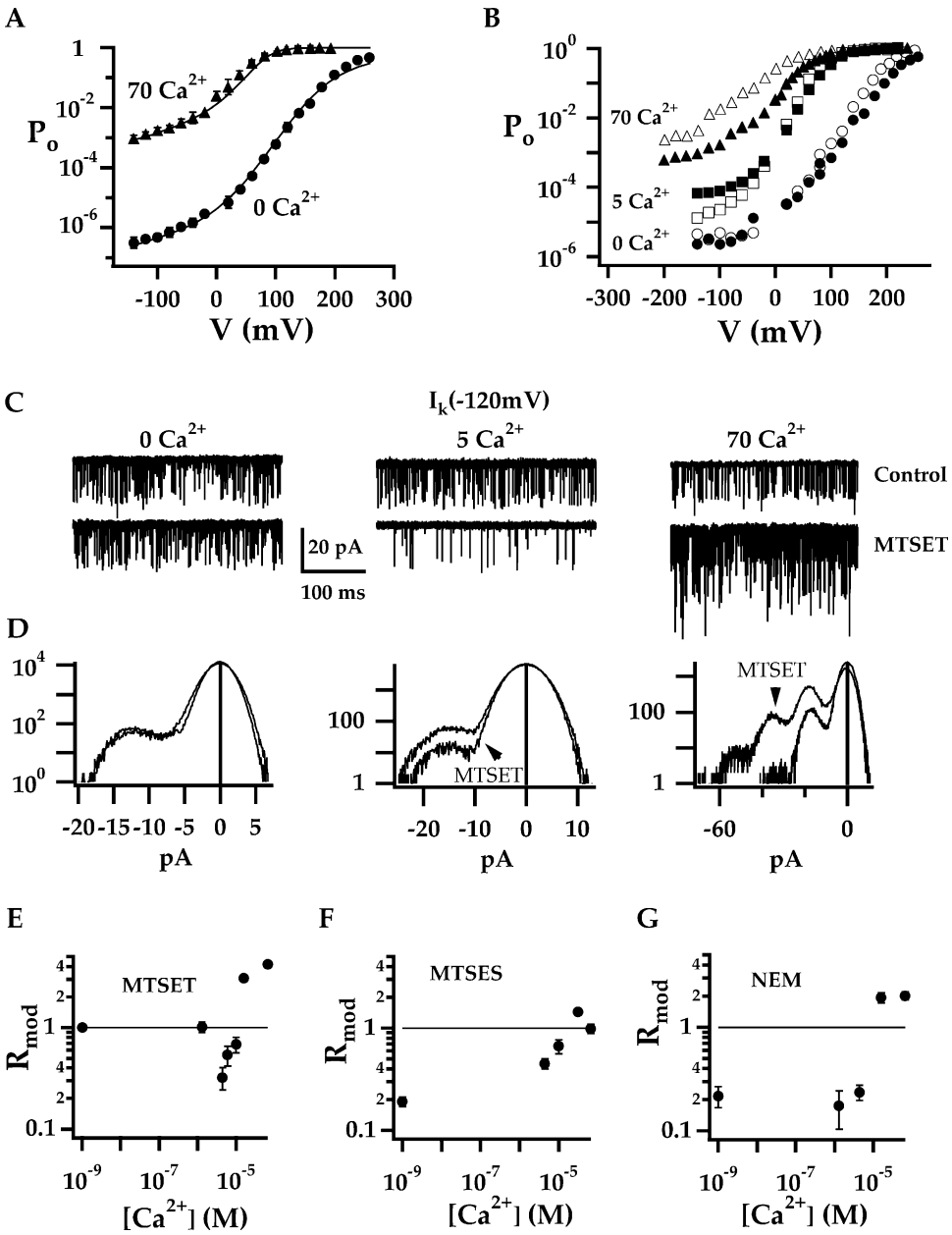

FIGURE 7. Cysteine modification alters steady-state activation at extreme negative voltages. (A) P_O–V relations (mean ± SEM) in 0 and 70 μM Ca^{2+}, plotted on a semi-log scale, show that steady-state activation is weakly voltage dependent and strongly Ca^{2+} dependent at extreme negative voltages. Lines are predictions of an allosteric model (Scheme I, Fig. 12 A) using B parameters in Table I. (B) P_O–V relations in 0, 5, and 70 μM Ca^{2+} measured in three different patches before (filled symbols) and after steady-state modification by MTSET (open symbols) indicate that MTSET alters the voltage dependence of steady-state activation. (C) Steady-state I_K recorded at −120 mV before (top) and after modification by MTSET (bottom) from the experiments in B. Patches contained hundreds of channels but unitary currents are observed at negative voltages because P_o is low. (D) Amplitude histograms corresponding to the data in C were obtained from 5-s recordings and indicate that P_o (−120) was unchanged in 0 Ca^{2+}, decreased in 5 μM Ca^{2+}, and increased in 70 μM Ca^{2+}. P_o at negative voltages was estimated as NP_O/N, where NP_o is determined from amplitude histograms and N is estimated from G_{Kmax} measured from macroscopic I_K (see MATERIALS AND METHODS). At more positive voltages, P_o was estimated as G_K/G_{Kmax}. (E–G) The effects of MTSET (E), MTSES (F), and NEM (G) on P_O (−120) at different [Ca^{2+}] are characterized by plotting the ratio $R_{mod} = NP_O$ (modified)/NP_O (control) at −120 mV (mean ± SEM).

gests that MTSET does not merely alter the energetics of channel opening.

To characterize the changes in gating that occur in the absence of voltage sensor activation, we determined the ratio $R_{mod} = P_O$(modified)/P_O(control) at −120 mV in various [Ca^{2+}] for MTSET, MTSES, and NEM. Steady-state currents were recorded at negative voltages before and after modification from macro-patches containing several hundred channels. Because P_O is small at −120 mV, single channel currents are observed (Fig. 7 C) and NP_o was determined from amplitude histograms (Fig. 7 D, see MATERIALS AND METHODS). In most cases, measurements were made at several voltages from −160 to −80 mV to confirm that NP_o is weakly voltage dependent at −120 mV. However, I_K at more positive voltages was often too large to record. Therefore, the number of channels in the patch (N) was not routinely determined, and R_{mod} was evaluated as NP_O(modified)/NP_O(control). To limit potential contributions of channel rundown to this ratio (e.g., a change in N), R_{mod} in each patch was determined at a single [Ca^{2+}], immediately before and after steady-state modification.

R_{mod} determined from many different patches (mean ± SEM) is plotted versus [Ca^{2+}] for MTSET (Fig. 7 E), MTSES (Fig. 7 F), and NEM (Fig. 7 G). In 0 Ca^{2+}, R_{mod} = 1 for MTSET, indicating that P_O(−120 mV) is un-

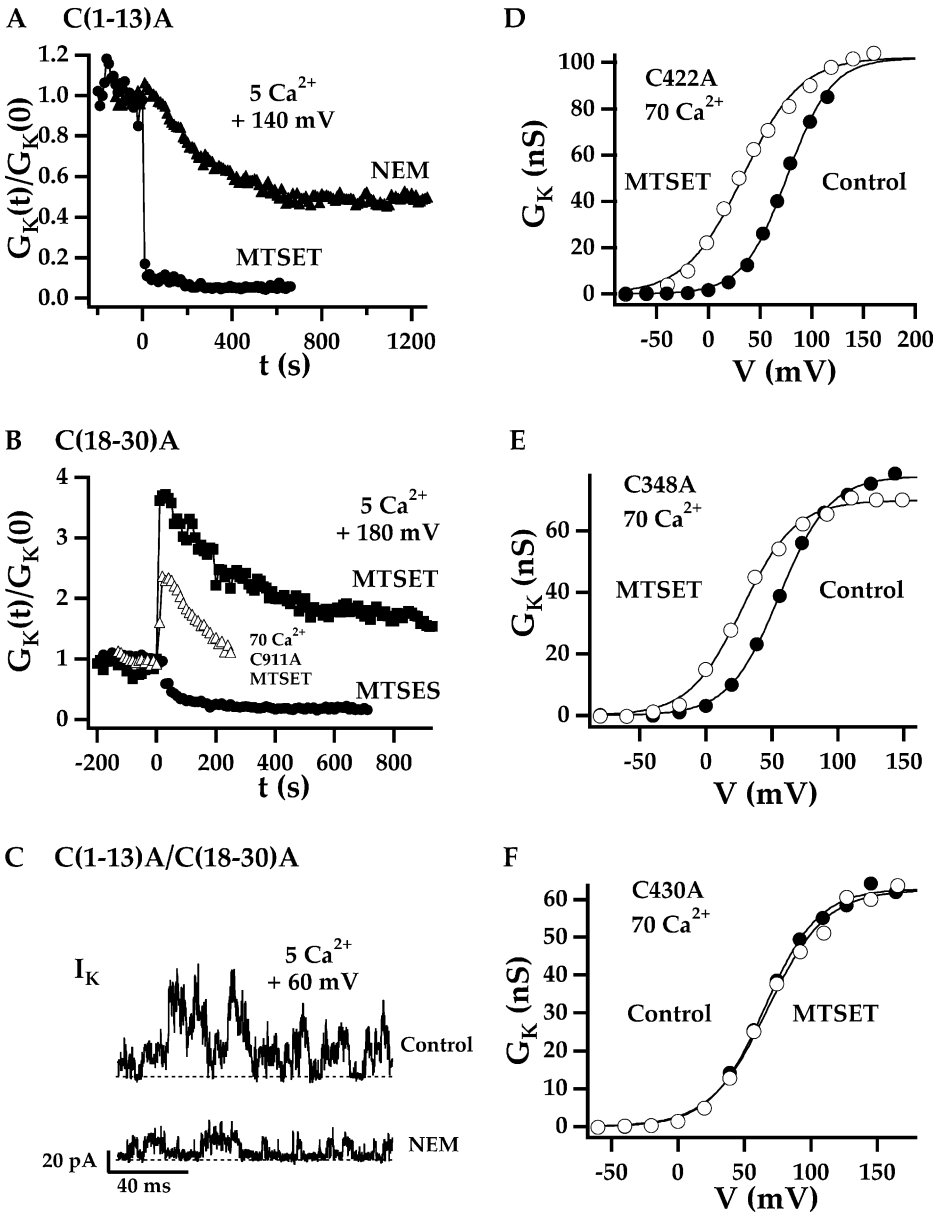

FIGURE 8. Identification of modification-sensitive cysteines. (A–C) Mutants of hSlo1 in which the first 13 and/or last 12 cysteines are replaced by alanine still respond to cysteine-modifying reagents. (A) G_K time course for C(1–13)A channels determined from 25-ms test pulses to +160 mV in 5 μM Ca^{2+} show a response to 100 μM MTSET or 20 mM NEM applied at $t = 0$ in two different patches. In both cases, I_K is reduced, indicating that one or more of the remaining cysteines (C14-C29) are modified. However, the response to MTSET differs from the WT (see text), suggesting that some of the removed cysteines may also be modification sensitive. (B) G_K time courses for C(18–29)A channels in 5 μM Ca^{2+} (V_{test} = +200 mV) also show a response to MTSET and MTSES that differs from the WT. The G_K time course for C911A in 70 μM Ca^{2+} is also plotted for MTSET. (C) Steady-state I_K recorded from C(1–13)A/C(18–29)A channels lacking both sets of cysteines, at +120 mV in 5 μM Ca^{2+} before and after treatment with 20 mM NEM for 300 s. NEM causes a marked decrease in channel activity, indicating that at least one of the four remaining cysteines (C14-C17) is sensitive to modification. (D–F) G_K–V relations in 70 μM Ca^{2+} before and after modification by MTSET are compared for three different point mutations at C7–C9 in the RCK1 domain (C348A, C422A, C430A). MTSET shifts the G–V for C348A (D) and C422A (E) to more negative voltages, like the WT. However, C430A (F) eliminates the effect of MTSET on the 70 μM Ca^{2+} G–V, indicating that C430 is an important site of modification.

changed. However, for MTSES and NEM, R_{mod} = 0.2, indicating that these reagents, unlike MTSET, inhibit channel opening in the absence of voltage sensor activation or Ca^{2+} binding. All three reagents also cause a decrease in P_O(−120 mV) at intermediate [Ca^{2+}] from ~1–10 μM (i.e., $R_{mod} < 1$). However, in higher [Ca^{2+}], P_O is increased by MTSET and to a lesser extent by NEM but is relatively unchanged by MTSES.

Although each reagent has distinct effects on P_O (−120 mV), they all enhance the response to Ca^{2+}. That is, the Ca^{2+}-dependent change in P_O from 0 Ca^{2+} to 70 μM Ca^{2+} at negative voltages is increased by cysteine modification. This effect is evident for MTSET from the P_o–V relations in Fig. 7 B. Moreover, that R_{mod} in 70 μM Ca^{2+} is always greater than R_{mod} in 0 Ca^{2+} indicates that this enhancement occurs for all three reagents (Fig. 7, E–G). Such an increase in the response to Ca^{2+} suggests that the coupling between Ca^{2+} binding and channel opening is strengthened by cysteine modification.

Identification of Modification-sensitive Cysteines

BK channel function is sensitive to modification of multiple cysteine residues (Tang et al., 2004). To identify these modification-sensitive residues, we examined the effects of MTSET, MTSES, and NEM on mutant constructs of hSlo1 that lack one or more cysteines. hSlo1 channels contain 29 cysteines, all of which are present

in mSlo1. Aside from an additional 56–amino acid COOH-terminal sequence including one cysteine present in mSlo1, hSlo1 shares 99% sequence identity with mSlo1 and exhibits similar functional properties (Brenner et al., 2000; Tang et al., 2001). The response of hSlo1 to cysteine-modifying reagents was not as extensively characterized as mSlo1. However, we tested the effects of MTSES and MTSET under many of the conditions described above for mSlo1 and observed no appreciable difference in terms of the direction and magnitude of changes in V_h and $P_O(-120)$ (unpublished data).

Initially, we examined several constructs in which multiple cysteines were replaced by alanine. When all 29 cysteines are replaced, channels express poorly and are difficult to study (Tang et al., 2004). However constructs lacking either the first 13 (C(1–13)A) or last 12 cysteines (C(18–29)A) express macroscopic currents. We tested the effects of MTSET, MTSES, and NEM on these two constructs in 5 μM Ca^{2+}. In both cases, G_K was greatly altered by modifying reagents (Fig. 8, A and B), indicating that modification-sensitive cysteines remain. Moreover, a construct in which both sets of cysteines were replaced by alanine (C(1–13)A/C(18–29)A) expressed poorly but exhibited a clear decrease in open probability in response to NEM (Fig. 8 C).

The ability of C(18–29)A to respond to both MTSET and MTSES (Fig. 8 B) is somewhat surprising, given that the same construct is reported to be insensitive to another MTS reagent (MTSEA), owing to the removal of a key cysteine at position 911 (Tang et al., 2004). We also examined the effect of MTSET on a point mutant C911A (Fig. 8 B) and observed a response similar to that of C(18–29)A. Thus, it is clear that modification of C911 cannot be solely responsible for the effects of MTSES and MTSET in the present study.

Although mutants were affected by cysteine-modifying reagents, their response was not identical to the wild type (WT). C(1–13)A G_K is decreased by NEM (Fig. 8 A), similar to the WT (Fig. 2 F). However MTSET decreases C(1–13)A G_K as opposed to an increase for the WT (Fig. 2 D). In contrast, G_K for C(18–29)A or C911A was immediately increased by MTSET (Fig. 8 B). However, this rapid increase was followed by a slow decay that is not observed with the WT. In addition, C(18–29)A G_K is decreased by MTSES in 5 μM Ca^{2+}, whereas WT G_K at the same $[Ca]_i$ is unaffected by MTSES (Fig. 2 B).

Differences in the response of WT, C(1–13)A, and C(18–29)A channels to cysteine-modifying reagents suggest that some of the removed cysteines may be modification sensitive. However, these differences are difficult to characterize and interpret owing to changes in channel function produced by the mutations. Both C(1–13)A and C(18–29)A required higher voltages to activate than the WT (Tang et al., 2004) and therefore could not be studied in the absence of Ca^{2+}. Given the complex interactions that occur between cysteine modification and channel function in the WT, it is possible that a change in gating caused by mutation could affect the response to cysteine modification. It is also possible that extensive mutation of cysteines could alter channel structure such that the accessibility of the remaining cysteines to modifying reagents is different than in the WT.

To minimize effects of mutation on channel structure or function, we examined the response to MTS reagents of several mutants where single cysteines were replaced. We focused on two regions in the COOH-terminal tail domain, the RCK1 domain and four central cysteines (C14-C17). The RCK1 domain is known to be functionally important and contains several cysteine residues, making it a likely candidate for modulation by cysteine modification. The response of C(1–13)A/C(18–29)A to NEM in Fig. 8 C suggests that at least one of the four remaining central cysteines may be modification sensitive in the WT. A cysteine residue was identified in each of these two regions that contribute significantly to the response to MTS reagents (Figs. 9 and 10).

C430 in the RCK1 Domain Underlies Multiple Effects of MTSES and MTSET

In the RCK1 domain, we tested the effect of MTSET on point mutants in which the first three cysteines (C7–C9) were replaced individually by alanine (C348A, C422A, C430A). G_K–V relations for all three mutants in 70 μM Ca^{2+} (Fig. 8, D–F) were similar to the WT (Fig. 3 A). Likewise, G_k evoked from C348A or C422A in 70 μM Ca^{2+} was rapidly increased by MTSET in a manner similar to the WT, producing a shift in the G–V relation to more negative voltages (Fig. 8, D and E). However C430A eliminated the effect of MTSET on the G–V in 70 μM Ca^{2+} (Fig. 8 F) and greatly reduced the effects of MTSET and MTSES at all $[Ca^{2+}]$ (Figs. 9 and 10).

G_K–V relations for C430A, in different $[Ca^{2+}]$ (Fig. 9 A), are similar to those of WT channels and exhibit similar V_h except at low $[Ca^{2+}]$ (<1 μM), where C430A is more difficult to activate and V_h is increased. The difference between V_h–$[Ca^{2+}]$ relations for WT and C430A (Fig. 9 B) resemble those produced by modification of the WT with MTSES (Fig. 6 F), suggesting that removal of C430 or its modification by MTSES may have similar effects on channel function. Consistent with the idea that MTSES acts primarily by modifying C430, C430A is almost insensitive to MTSES. In 0 Ca^{2+}, MTSES decreases WT G_K by 80% but has no detectable effect on C430A under the same conditions (Fig. 9 C). Similarly, MTSES had no significant effect on the V_h–$[Ca^{2+}]$ relation for C430A (Fig. 9 E). Likewise, MTSES produced little change in $P_o(-120)$ for C430A (i.e., $R_{mod} \sim 1$; see Fig. 12 C).

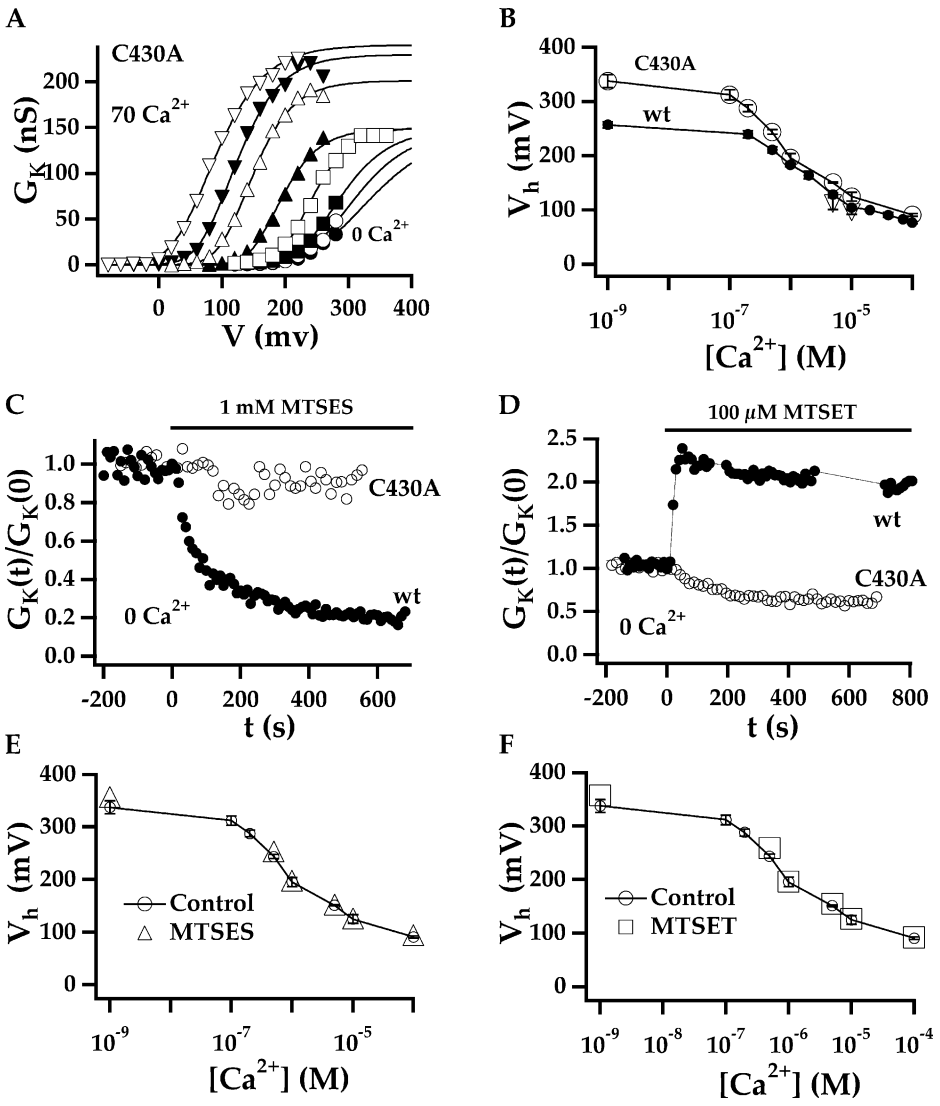

FIGURE 9. C430A reduces the response to MTSES and MTSET. (A) G_K–V relations for C430A channels in different $[Ca^{2+}]$ from a single patch (0 [●], 0.1 [○], 0.3 [■], 0.6 [□], 1.3 [▲], 4.4 [△], 10 [▼], 66 [▽]). (B) V_h–$[Ca^{2+}]$ relations (mean ± SEM) are compared for WT mSlo1 (●), hSlo1 (▽), and C430A (○) channels, indicating that C430A G–Vs are shifted to more positive voltages than the WT at low $[Ca^{2+}]$. (C) MTSES decreases WT G_K (●) in 0 Ca^{2+} (from Fig. 2 B) but has no detectable effect on C430A G_K (○) under the same conditions (V_{test} = +200 mV). (D) MTSET rapidly increases WT G_K (●) in 0 Ca^{2+} (From Fig. 2 D), but decreases C430A G_K (○) under the same conditions (V_{test} = +200 mV). (E and F) V_h–$[Ca^{2+}]$ relations (mean ± SEM) for C430A before (○) and after treatment with 1 mM MTSES for 300 s (△) or 100 μM MTSET for 30 s (□) are almost indistinguishable. For clarity, only mean V_h is shown after modification, but variance was similar to the control.

Mutation of C430 reduces, but does not eliminate, effects of MTSET on channel gating. In 0 Ca^{2+}, MTSET produces a rapid increase in WT I_K, but C430A exhibits a slow decrease (Fig. 9 D). V_h for the mutant also increases slightly in 0 Ca^{2+} although no change in V_h is detected at higher $[Ca^{2+}]$ (Fig. 9 F). Although C430A almost abolishes the effects of MTSET on V_h, it does not eliminate changes in $P_O(-120)$ (Fig. 10 A). Similar to the WT, $P_O(-120)$ for C430A is unaffected by MTSET in 0 Ca^{2+} but is markedly decreased in 10 μM Ca^{2+} (Fig. 10 A). In contrast, MTSET has no effect on $P_O(-120)$ in 70 μM Ca^{2+} (Fig. 10 A), whereas the WT shows an approximate fivefold increase (Fig. 7 C). G_K–V relations for C430A measured from individual patches immediately before and after treatment with MTSET confirm that there is little change in V_h in 10 or 70 μM Ca^{2+} and a small change in 0 Ca^{2+} (Fig. 10 B).

The differences in the response of WT and C430A channels to MTSET suggest that modification of C430 by MTSET may act to both increase $P_O(-120$ mV) in the presence of Ca^{2+} and shift the G_K–V relations to more negative voltages. At intermediate $[Ca^{2+}]$, an increase in $P_O(-120)$ produced by modification of C430 could be masked by a decrease in $P_O(-120)$ produced by modification of an additional site. This hypothesis is supported by the observation that the decrease in $P_O(-120)$ produced by MTSET in 10 μM Ca^{2+} is at least twofold greater for C430A than for the WT (see Fig. 12 E).

C615 in the Heam-binding Site Is Sensitive to MTSET

The response of C(1–13)A/C(18–29)C to NEM (Fig. 7 C) suggests that at least one of four remaining cysteines in this construct (C612, C615, C628, C630) is also important for the effects of cysteine modification. We examined the effect of point mutations in three of these residues. Since the C430 site appears responsible in large part for changes in V_h and increases in

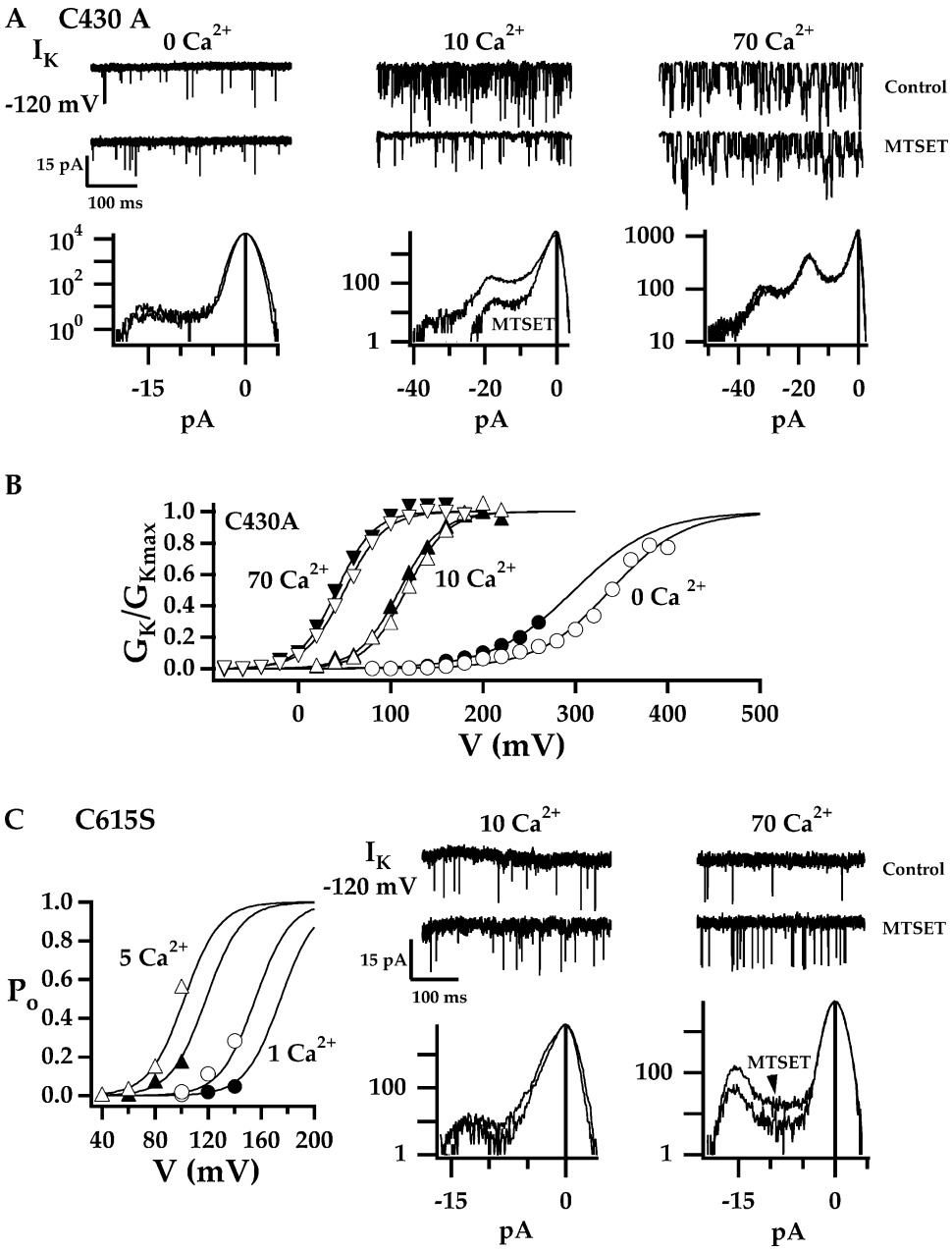

FIGURE 10. C430A and C615S alter effects of cysteine modification on P_o at negative voltages. (A) Steady-state I_K at −120 mV (top) for C430A channels from three patches in different [Ca^{2+}] before and after treatment with 100 μM MTSET for 60 s. Corresponding amplitude histograms (bottom) determined from 20-s recordings indicate that P_o is relatively unchanged in 0 Ca^{2+} and decreased in 10 μM Ca^{2+}, similar to the WT. However, C430A eliminates the increase in $P_o(-120)$ observed for the WT in 70 μM Ca^{2+}. (B) G_K–V relations for C430A measured from three different patches immediately before (0 [●], 10 [■], 70 [▼]) and after treatment with MTSET (0 [○], 10 [□], 70 [▽]), confirm results from mean V_h (Fig. 9 F) that there is little change in V_h even at 10 μM Ca^{2+} where $P_o(-120$ mV) is reduced. (C) P_o–V relations for C615S (left) from a single patch in 1 μM Ca^{2+} and 5 μM Ca^{2+} are both shifted by approximately −20 mV following treatment with MTSET. The patch contained five channels, and P_o was determined from 10-s steady-state recordings. Boltzmann fits (lines) were constrained to have the same apparent charge ($z = 0.72$ *e*). Steady-state I_K at −120 mV (right) for C615S from two patches in different [Ca^{2+}] before and after treatment with 100 μM MTSET. Amplitude histograms indicate that P_o increases in 70 μM Ca^{2+}, like the WT. However, C615S eliminates the decrease in P_o (−120) observed for the WT in 10 μM Ca^{2+}.

$P_O(-120)$ in high Ca^{2+}, we screened for the ability of MTSET to decrease $P_O(-120)$ in 10 μM Ca^{2+}. C628S and C630S both exhibited substantial decreases in $P_O(-120)$ like the WT channel (unpublished data). However C615S, in the Heam-binding site, eliminated this effect of MTSET (Fig. 10 C, middle). Despite a decreased response to MTSET in 10 μM Ca^{2+}, C615S still exhibits a marked increase in $P_O(-120)$ in 70 μM Ca^{2+} (Fig. 10 C, left). Similarly, P_o–V relations in 1 and 5 μM Ca^{2+} were shifted to more negative voltages (Fig. 10 C, right). These results are consistent with the assumption that decreases in V_h and increases in $P_O(-120)$ in 70 μM Ca^{2+} reflect modification of C430 by MTSET.

Deletion of the RCK1 αD–βD Linker Enhances Channel Activation

The sensitivity of C430 to modification and mutation suggests that this residue and/or nearby residues in the RCK1 domain play important roles in channel gating. The RCK1 domain is thought to have a Rossmann-fold topology containing a series of alternating α-helices and β-sheets (Jiang et al., 2001). Alignment of BK channel sequences with RCK domains of known structure indicate that C430 is located between α-helix D (αD) and β-sheet D (βD) (Jiang et al., 2001, 2002). Fig. 11 A compares the sequences of mSlo1, hSlo1, and the fly homologue dSlo1 in this region with that of the MthK chan-

nel based on an alignment from Jiang et al. (2002) of BK channels with eight prokaryotic channels and transporters containing RCK domains. The αD–βD linker of MthK and other prokaryotic RCK domains contains only two amino acids. However BK channels contain an additional eight–amino acid domain including C430. The absence of this domain from the prokaryotic channels suggests it is not critical to RCK domain structure. Yet its sequence is highly conserved among BK channels, suggesting a possible functional role.

To examine the role of the αD–βD linker, we deleted the extra eight–amino acid domain from hSlo1 (hSlo1-ΔD, Fig. 11 A) and compared its function to that of the WT. Like the WT, hSlo1-ΔD exhibited robust expression and responded rapidly to changes in voltage or Ca^{2+} (not depicted), consistent with the notion that the deletion does not radically disrupt channel structure. Likewise, G_K–V relations were similar in shape to the WT and exhibit a large shift in response to Ca^{2+} (Fig. 11 B). However, the G_K–V relations in 0 Ca and 70 μM Ca^{2+} were shifted by −84 and −101 mV, respectively, relative to the WT. That is, hSlo1-ΔD was much easier to activate. This difference does not reflect a change in rundown (i.e., oxidation) caused by removal of C430 since the G–Vs for C430A (Fig. 9 B) and hSlo1-ΔD were shifted in opposite directions relative to the WT. WT, hSlo1-ΔD, and C430A channels all exhibited time-dependent shifts of the G–V to more positive voltages and were studied a similar time after patch excision. Thus, the αD–βD linker has a large impact on channel gating, suggesting that effects of C430 modification could to some extent reflect perturbation of neighboring residues in the linker and/or the interaction of linker residues with the rest of the channel.

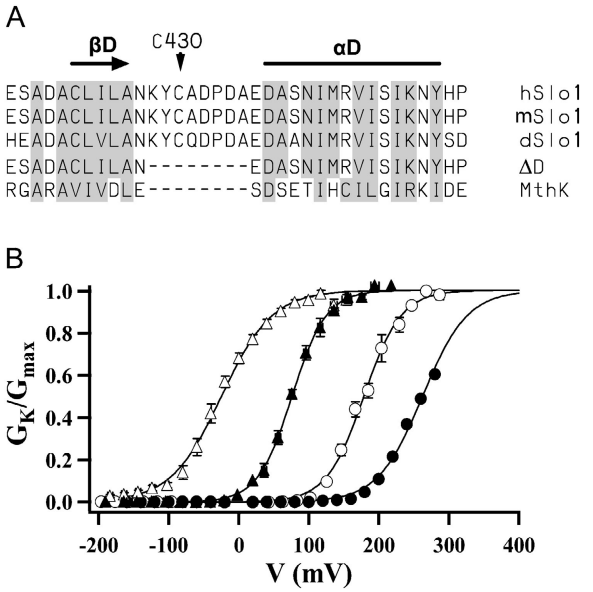

FIGURE 11. Deletion of the αD–βD linker in the RCK1 domain enhances channel activation. (A) Amino acid sequence comparison of the MthK channel with BK channel homologues for human (hSlo1), mouse (mSlo1), and fly (dSlo1) as well as a deletion construct (hSlo-ΔD), covering the αD–βD region of the RCK1 domain. Alignments are taken from Jiang et al. (2002) and based on comparison of RCK domains for hSlo1, dSlo1, and eight prokaryotic channels and transporters including MthK. Shaded residues are semiconserved among the aligned sequences. Locations of αD and βD are from the MthK crystal structure. Eight amino acids, present in BK channels but absent in MthK, were deleted from hSlo1 to make the hSlo-ΔD construct. (B) Mean G_K–V relations for hSlo1 (●, ▲) and hSlo-ΔD (○, Δ) are compared in 0 Ca^{2+} (circles) and 70 μM Ca^{2+} (triangles). Lines are fits to Boltzmann functions (0 Ca^{2+}: hSlo1 V_h = 262 mV, z = 0.79 *e*, hSlo-ΔD V_h = +179 mV, z = 0.95 *e*; 70 μM Ca^{2+}: hSlo1 V_h = +76 mV, z = 1.03 *e*, hSlo-ΔD V_h = −25 mV, z = 0.70 *e*).

DISCUSSION

We have studied the effects of cysteine-modifying reagents on native cysteines in the BK channel α-subunit to identify regions of the large COOH-terminal tail domain that influence channel function and to understand the gating mechanisms that are influenced by these regions. A similar strategy for structure–function analysis would involve mutating random sites within the tail domain. However, our approach has the advantage that modification of native cysteines is already known to impact channel gating and that we are able to compare changes in function before and after cysteine modification in the same patch. BK channels exhibit significant patch-to-patch variation in gating properties that can complicate the comparison of subtle differences between mutant and WT channels.

Our results demonstrate that the effects of cysteine-modifying reagents on BK channel function are complex in terms of the changes in channel gating, sensitivity to different modifying adducts, and sites of action. We have identified two cysteine residues whose removal reduces the effects of MTS reagents. C430 in the RCK1 domain appears to be particularly important, as its removal almost abolishes the effect of MTSES and greatly alters that of MTSET. C615 in the Heam-binding site also has a significant effect on the action of MTSET. As discussed below, modification of C430 and C615 has distinct effects on channel gating mechanisms, and the modification of multiple cysteines, including C911 recently described by Tang et al. (2004), is likely to account for the complexity of cysteine-modification effects.

The sensitivity of C430 and C615 to modification implies that these cysteines and/or nearby parts of the channel play a role in gating. In the case of C615, this is interesting because the residue lies in the Heam-binding site and the functional perturbations caused by cysteine modification may therefore be relevant to the modulatory effects of Heam binding. In the case of C430, modifying reagents cause multiple effects on

function that can be related mainly to the coupling between Ca^{2+} binding and voltage sensor activation and channel opening. Deletion of a unique sequence including C430 in the RCK1 domain also has significant impact on function. These results are relevant to understanding the role of the RCK domain in BK channel gating.

MTSET, MTSES, and NEM appear to modify the same residues based on the ability of pretreatment with one to prevent the effect of another. However, each reagent has a distinct effect on channel function. MTSES and NEM shift the G–V to more positive voltages, whereas MTSET shifts the G–V in the opposite direction. NEM and MTSES reduce $P_O(-120)$ dramatically in 0 Ca^{2+}, whereas MTSET has no effect on $P_O(-120)$ under the same conditions. In general, changes in P_O induced by each reagent exhibit a different profile of Ca^{2+} and voltage dependence. Moreover, conditions exist where each reagent has little effect on steady-state activation. NEM does not change V_h in 0 Ca^{2+} or 70 μM Ca^{2+}. MTSET has little effect on V_h over a narrow range of intermediate Ca^{2+} near 1 μM. MTSES has no effect on V_h for $[Ca^{2+}] > 1$ μM. Failure to observe a change in steady-state activation under these conditions does not represent a failure to modify cysteines. The changes in channel function produced by each reagent were not dependent on the conditions under which the modifying reagents were applied. Rather, under certain conditions of $[Ca^{2+}]$ and voltage, changes in gating do not manifest as a change in steady-state activation. In some cases, changes in I_K kinetics were observed when V_h was unchanged.

It is not surprising that conditions exist where cysteine modification leaves P_o unchanged. For example, if Ca^{2+} binding is altered by modification, then channel gating in the absence of Ca^{2+} should be unchanged (Tang et al., 2004). Likewise, if voltage sensor movement is altered, P_o should be unchanged at negative potentials where voltage sensors are not activated. In addition, it is likely that modification of multiple cysteines can have opposing effects on gating that cancel out and leave P_o unchanged over a narrow range of conditions. For example, MTSET in 5 μM Ca^{2+} leaves P_o unchanged near 0 mV while increasing $P_o(V_h)$ and decreasing $P_o(-120$ mV) (Fig. 7 B). In this case, the lack of a change near 0 mV probably reflects the opposing effects of modifying C430 and C615, because mutation of these sites almost abolishes the effects on P_o at V_h and −120 mV, respectively. That MTSET leaves V_h unchanged over a relatively narrow range of $[Ca^{2+}]$ (0.5–2 μM) is also likely to reflect action at multiple cysteines.

Mechanisms of Action

The activation of BK channels by Ca^{2+} and voltage can be described in terms of allosteric mechanisms (Horrigan and Aldrich, 2002). Channels undergo a closed to open (C-O) conformational change that occurs with low probability in the absence of Ca^{2+} and voltage sensor activation. Opening does not require Ca^{2+} binding or voltage sensor activation but is enhanced by either. That is, Ca^{2+} and voltage act almost independently to increase P_O.

To understand how these gating mechanisms are perturbed by cysteine modification, we examined changes in steady-state activation produced by MTSET, MTSES, and NEM over a wide range of $[Ca^{2+}]$ and voltage. These conditions include $[Ca^{2+}]$ where high-affinity Ca^{2+}-binding sites should be vacant or saturated, and negative potentials that should force voltage sensors into a resting state. The changes in channel function produced under these limiting conditions in many cases provide a direct indication of the changes in gating mechanism.

That all three reagents alter channel function in the absence of Ca^{2+} indicates that none act merely to perturb Ca^{2+} binding. In 0 Ca^{2+}, V_h is altered by MTSET or MTSES, and $P_O(-120$ mV) is decreased markedly by MTSES or NEM. The decreases in $P_O(-120)$ indicate that the C-O equilibrium constant is reduced in the absence of Ca^{2+} binding or voltage sensor activation. The ability of MTSET to alter V_h without changing $P_O(-120)$ implies that voltage-dependent gating must also be modified. That MTSET alters $P_O(-120)$ only in the presence of Ca^{2+} indicates that Ca^{2+}-dependent gating must also be modified. Taken together, these results under limiting conditions indicate that many aspects of the gating mechanism are altered by cysteine modification. Thus, it is not surprising that modifying reagents produce complicated changes in the Ca^{2+} and voltage dependence of P_o under nonlimiting conditions where voltage, Ca^{2+} binding, and the energetics of the C-O transition all contribute to steady-state activation.

Modeling Changes in Steady-state Activation

To quantify changes in the gating mechanism and to account for results under nonlimiting conditions, we compared the changes in V_h and $P_O(-120$ mV) at various $[Ca^{2+}]$ to the predictions of an allosteric model (Fig. 12). The model (Fig. 12 A, Scheme I), used previously to describe the ionic and gating currents of mSlo1 (Horrigan and Aldrich, 2002), includes a closed–open (C-O) conformational change characterized, in the absence of Ca^{2+} and voltage sensor activation, by an equilibrium constant L_o and charge z_L. Voltage sensors in each of four identical subunits are represented by a resting to activated (R-A) conformational change with an equilibrium constant J_0 and charge z_J. Ca^{2+} binding is depicted as four identical binding sites that equilibrate between Ca^{2+}-free (X) and bound

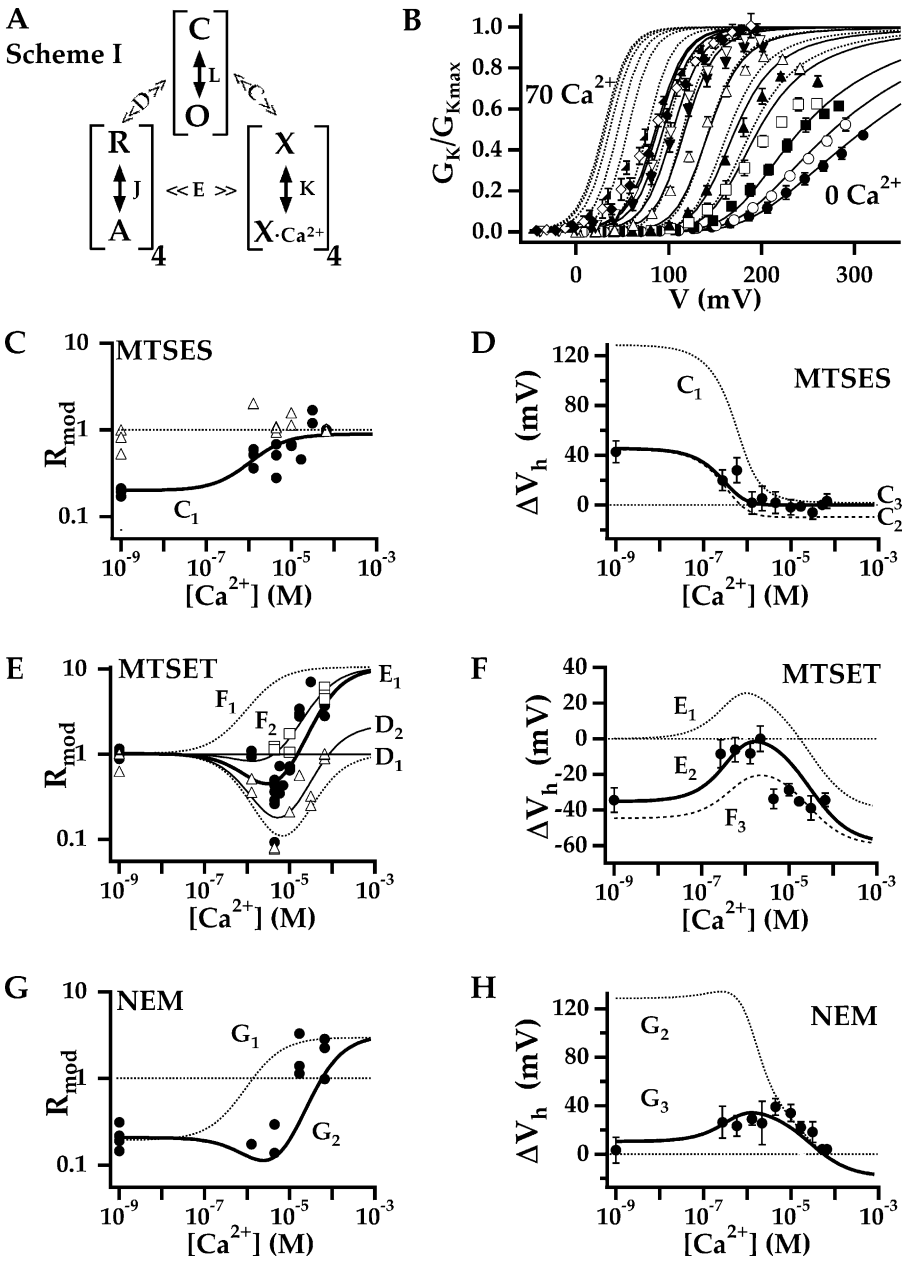

FIGURE 12. Modeling the effects of cysteine modification. (A) Scheme I, an allosteric model of BK channel gating includes a closed to open conformational change (C-O) that is influenced by activation of four identical voltage sensors that can be in resting or activated states (R, A), and four identical binding sites that can be vacant (X) or occupied by Ca^{2+} (X-Ca^{2+}) (see text for details). (B) G_K–V relations (mean ± SEM) for mSlo1 in different [Ca^{2+}] (in μM: 0 [●], 0.3 [○], 0.6 [■], 1.3 [□], 2 [▲], 4.4 [△], 10 [▼], 17 [▽], 31 [◆], 51 [◇], 66 [◢]) represent data in Fig. 6 A that have been normalized to G_{Kmax} in 70 μM Ca^{2+}. Lines are predictions of Scheme I using parameter sets A (dashed) or B (solid) from Table I. (C, E, and G) R_{mod}–[Ca^{2+}] relations for MTSES, MTSET, or NEM (symbols) are plotted together with predictions of Scheme I (lines) using the indicated parameter sets from Table I. R_{mod} = NP_o (modified)/NP_o (control) at −120 mV. Each data point represents a different patch involving either WT (●), C430A (△), or C615S (□) channels. (D, F, and H) ΔV_h–[Ca^{2+}] relations (mean ± SEM) for WT channels are compared with the predictions of Scheme I (lines).

(X-Ca^{2+}) states with second order equilibrium constant $K = [Ca^{2+}]/K_D$. K_D is the dissociation constant for Ca^{2+} when the channel is closed. The interaction between Ca^{2+} binding and channel opening is represented by an allosteric factor C where the C-O equilibrium increases C-fold for each Ca^{2+} bound. The interaction of voltage sensor activation with channel opening is represented by an allosteric factor D where the C-O equilibrium constant increases D-fold for each voltage sensor activated. A weak interaction between Ca^{2+} binding and voltage sensor activation (E) is also included (Horrigan and Aldrich, 2002). The equilibrium properties of this gating mechanism are fully described by eight parameters:

$$P_o = \frac{L(1 + KC + JD + JKCDE)^4}{L(1 + KC + JD + JKCDE)^4 + (1 + J + K + JKE)^4}, \quad (1)$$

where

$$L = L_0 \exp\left(\frac{z_L V}{kT}\right);$$

$$J = J_0 \exp\left(\frac{z_J V}{kT}\right);$$

$$K = \frac{[Ca^{2+}]}{K_D}.$$

Before modeling the effects of cysteine modification, parameters were determined for the control data. As noted above, G–Vs were shifted to more positive volt-

ages relative to previous studies and exhibit an apparent decrease in G_{Kmax} at low Ca^{2+}. Mean G_k–V relations for mSlo1 are plotted in Fig. 12 B together with predictions of the model using parameters from a previous study (dashed lines; Table I, A parameters) and with the parameters adjusted to fit the data (solid lines; Table I, B parameters). A decrease in D from 25 to 12, representing a 23% reduction in the energy of coupling between voltage sensor activation and channel opening, was sufficient to reproduce both the positive shift in V_h and the shape of the G–V in 0 Ca^{2+}. A similar effect can also be produced by decreasing L_0 15-fold (unpublished data). However, such a reduction in the C-O equilibrium constant is not consistent with $P_o(-120)$, as discussed below; and only minor adjustments were made to L_o and C while K_D, z_L, z_J, and J_o were left unchanged. The only other significant adjustment was a decrease in E that had no effect on the G—V in 0 Ca^{2+} and little impact in high Ca^{2+} but improved fits at intermediate [Ca^{2+}] where the model otherwise predicts a greater sensitivity to Ca^{2+} than is actually observed. E is best determined by gating current measurements that were not performed in the present study (Horrigan and Aldrich, 2002). Therefore E was decreased from 2.4 to 1, to eliminate the weak interaction between Ca^{2+} binding and voltage sensor activation and simplify the model.

The model does not predict that G_{Kmax} decreases in low Ca^{2+} but rather that the slope of the G–V is reduced such that G_{max} is not achieved until extreme positive voltages. In practice, we cannot distinguish between this prediction and the data given that the apparent saturation of G_K in low Ca^{2+} depends on measurements at very positive voltages, near +300 mV. Channel block by trace metal ions such as Ba^{2+} might influence such measurements (Diaz et al., 1996; Neyton, 1996; Cox et al., 1997b), although a Ba^{2+} chelator was included in the internal solution to minimize blocking effects (see MATERIALS AND METHODS).

Despite differences between the present and previous data, there are also similarities that indicate most parameters are unchanged. The Ca^{2+} dependence of V_h is similar to previous studies (Fig. 9 B), suggesting that parameters associated with Ca^{2+}-dependent gating (K_D, C) are similar. Moreover, P_o at negative voltages was almost identical to previous measurements (Horrigan et al., 1999; Horrigan and Aldrich, 2002). L_o was only adjusted slightly to fit the P_o–V relation in 0 Ca^{2+} (line, Fig. 7 A). The model reproduces not only the magnitude of $P_o(-120)$ but also the voltage dependence of P_o, supporting the assumption that the charge associated with channel opening (z_L) as well as parameters associated with voltage sensor activation (z_J, J_0) are not altered. The allosteric factor C was adjusted slightly to fit the large increase in $P_o(-120)$ between 0 and 70 μM Ca^{2+} (lines, Fig. 7 A). The K_D for Ca^{2+} was left unchanged because the increase in mean $P_o(-120)$ between 0 and 4.4 μM Ca^{2+} was 145 ± 55-fold (mean ± SEM, $n = 3$), not significantly different than the 100-fold change predicted by the model.

TABLE I

Scheme I: Parameters

	L_0	K_D	C	D	J_0	E
(A) WT	9.8×10^{-7}	11 μM	8	25	0.032	2.4
(B) WT	1.3×10^{-6}	11 μM	8.6	12	0.032	1
(C_1) WT + MTSES	2.6×10^{-7}	11 μM	12.5	12	0.032	1
(C_2) WT + MTSES	2.6×10^{-7}	11 μM	12.5	15.5	0.032	1
(C_3) WT + MTSES	2.6×10^{-7}	11 μM	12.5	15	0.024	1
(D_1) C430A + MTSET	1.3×10^{-6}	35 μM	8.6	12	0.032	1
(D_2) C430A + MTSET	1.3×10^{-6}	35 μM	10.5	12	0.032	1
(E_1) WT + MTSET	1.3×10^{-6}	35 μM	15.5	12	0.032	1
(E_2) WT + MTSET	1.3×10^{-6}	35 μM	15.5	14	0.045	1
(F_1) C615S + MTSET	1.3×10^{-6}	11 μM	15.5	12	0.032	1
(F_2) C615S + MTSET	1.3×10^{-6}	25 μM	15.5	12	0.032	1
(F_3) C615S + MTSET	1.3×10^{-6}	25 μM	15.5	14	0.045	1
(G_1) WT + NEM	2.6×10^{-7}	11 μM	17	12	0.032	1
(G_2) WT + NEM	2.6×10^{-7}	35 μM	17	12	0.032	1
(G_3) WT + NEM	2.6×10^{-7}	35 μM	17	17.5	0.020	1

For all fits, $z_L = 0.3$ *e*, $z_J = 0.58$ *e*.

Modeling the Effects of Cysteine Modification

Once parameters were adjusted to fit the control data, we determined which parameters could be changed to reproduce the effects of cysteine-modifying reagents. Fig. 12 (C, E, and G) plots the R_{mod}–[Ca^{2+}] relations for MTSES, MTSET, and NEM, respectively, for WT and mutant channels, where $R_{mod} = NP_O$ (modified)/NP_O(control) at −120 mV. Individual data points are plotted, as opposed to averages, in Fig. 9, because different numbers of measurements were made at each [Ca^{2+}] and each point represents a different patch. Fig. 12 (D, F, and H) plots the G_K–V shift (ΔV_h) produced by channel modification (mean ± SEM), equivalent to the difference between control and modified V_h–[Ca^{2+}] relations in Fig. 6. Based on the similar shape of G_K–V relations in high [Ca^{2+}] before and after modification (Fig. 3 A; Fig. 6 E; Fig. 7 B; Fig. 8 F), we conclude that the charge associated with voltage sensor activation (z_J) or channel opening (z_L) is not altered, leaving six parameters that can be adjusted (L_o, K_d, C, D, E, and J_0). Although R_{mod} exhibits considerable scatter, we focused on fitting this data first because only three free parameters (L_o, K_d, and C) influence $P_O(-120)$.

The Effects of MTSES

MTSES decreases $P_O(-120)$ fivefold in 0 Ca^{2+} (i.e., $R_{mod} = 0.2$), indicating a fivefold decrease in the C-O equilibrium constant L_o. A decrease in L_o by itself

should reduce $P_O(-120)$ at all $[Ca^{2+}]$ equally. However, R_{mod} is smallest in 0 Ca^{2+} and approaches unity in high Ca^{2+}. To reproduce a Ca^{2+}-dependent increase in R_{mod} requires that the allosteric factor C be increased. Together, a decrease in L_o and increase in C reasonably approximate the R_{mod}–Ca^{2+} relationship (solid line, Fig. 12 C; Table I, C_1) and predict the shape, although not the magnitude, of the ΔV_h–$[Ca^{2+}]$ relation (Fig. 12 D, C_1), including that V_h is altered only at very low $[Ca^{2+}] < 1$ μM. The magnitude of the ΔV_h–$[Ca^{2+}]$ relation can be reproduced without altering the R_{mod}–$[Ca^{2+}]$ relation by increasing the allosteric factor D (Fig. 12 D, C_2; Table I, C_2). The fit is further improved in high Ca^{2+} if the voltage sensor equilibrium constant J_0 is decreased slightly (Fig. 12 D, C_3; Table I, C_3). The mutant C430A shows little response to MTSES (Fig. 11 C; Fig. 10 E), implying that changes in L_o, C, D, and J_0 used to fit the WT data reflect modification of C430.

The Effects of MTSET

MTSET has effects on R_{mod} (Fig. 12 E) and ΔV_h (Fig. 12 F) that differ from those of MTSES and involve action at more than one cysteine residue. However, as shown below, MTSET shares with MTSES an ability to increase C and D by modifying C430.

That MTSET modifies residues in addition to C430 is evident from the marked decrease in R_{mod} produced at intermediate $[Ca^{2+}]$ for C430A (Fig. 12 E). Such an effect is consistent with a decrease in Ca^{2+} affinity such that Ca^{2+} bound at intermediate $[Ca^{2+}]$ is decreased whereas Ca^{2+} occupancy in 0 Ca^{2+} and saturating Ca^{2+} are unchanged. The model predicts a U-shaped R_{mod}–$[Ca^{2+}]$ relation when K_D is increased from 11 to 35 μM without changing other parameters (Fig. 12 E, D_1; Table I, D_1). This approximates the 10-fold decrease in R_{mod} near 5 μM Ca^{2+} for C430A, but underestimates R_{mod} at high Ca^{2+}. An improved fit can be obtained by increasing C slightly from 8.6 to 10.5 (Fig. 12 E, D_2; Table I, D_2). Similarly, the WT data can be fit by further increasing C to 15.5 with K_D = 35 μM (Fig. 12 E, E_1; Table I, E_1). The increase in C appears sufficient to account for the difference between the response of C430A and WT, implying that modification of C430 increases C. The mutation C615S eliminates the change in R_{mod} at 5 μM Ca^{2+} but not in high Ca^{2+}, suggesting that modification of C615 increases K_D with little effect on C. However, C615 is not solely responsible for the change in K_D. If we assume that MTSET acts only to increase C, then the model predicts R_{mod} will increase over a 10-fold lower Ca^{2+} range than is actually observed for C615S (Fig. 12 E, F_1; Table I, F_1). The data can be fit by assuming K_D is increased to 25 μM (Fig. 12 E, F_2; Table I, F_2). That is, modification of a site other than C615 or C430 increases K_D from 11 to 25 μM, and modification of C615 must further increase K_D to 35 μM to account for the response of the WT. A possible candidate for the additional site as discussed below is C911 described by Tang et al. (2004).

The parameters that fit the R_{mod}–$[Ca^{2+}]$ relation for the WT channel also reproduce the basic shape of the ΔV_h–$[Ca^{2+}]$ relation (Fig. 12 F, E_1; Table I, E_1) but overestimate ΔV_h, especially in 0 Ca^{2+}. That the G–V is shifted in 0 Ca^{2+} ($\Delta V_h = -34 \pm 7$ mV) although $P_O(-120)$ is not changed ($R_{mod} = 1.00 \pm 0.05$) indicates that voltage-dependent gating must be altered. The data can be fit by increasing D and J_0 (Fig. 12 F, E_2; Table I, E_2). As in the case of MTSES, the increase in D was necessary to fit ΔV_h in 0 Ca^{2+}, whereas the adjustment of J_0 had a smaller effect. A similar ΔV_h–$[Ca^{2+}]$ relation is predicted for C615S (Fig. 12 F, F_3; Table I, F_3), with the difference that ΔV_h is always negative for the mutant, consistent with the approximate −20-mV G–V shifts observed for 1 and 5 μM Ca^{2+} in Fig. 10 C.

Although the C430A mutant exhibits a marked decrease in $P_o(-120)$ at intermediate $[Ca^{2+}]$, it exhibits little or no change in V_h in response to MTSET (Fig. 9 F). That V_h and $P_O(-120)$ don't change for C430A in 0 Ca^{2+} and saturating Ca^{2+} is consistent with the increases in C and D used to fit the WT response being caused by modification of C430. However, the failure of V_h to change at all $[Ca^{2+}]$ is not readily explained by the model since an increase in K_D used to fit the R_{mod}–$[Ca^{2+}]$ relation generally predicts a bell-shaped ΔV_h–$[Ca^{2+}]$ relation. One factor that may influence our ability to fit the mutant data is that effects of cysteine modification on C430A or C615S were modeled using control parameters identical to those of the WT. This may be an oversimplification because V_h–$[Ca^{2+}]$ relations for WT and C430A differ in low $[Ca^{2+}]$ (Fig. 9 B). However, mutants were not as well characterized as the WT and not all control parameters could be determined.

The Effects of NEM

The effect of NEM on $P_O(-120)$ resembles that of MTSES with $R_{mod} = 0.2$ in 0 Ca^{2+} and increasing at higher $[Ca^{2+}]$ (Fig. 12 G). These effects imply that NEM, like MTSES, decreases L_o and increases C. When L_o is decreased fivefold and C is increased twofold, the model approximates R_{mod} in 0 Ca^{2+} and high $[Ca^{2+}]$ (Fig. 12 G, G_1; Table I, G_1). However, the model also predicts that R_{mod} will increase rapidly near $[Ca^{2+}] = 1$ μM, as for MTSES (Fig. 12 C), whereas the data increases over a 10-fold higher Ca^{2+} range, suggesting that K_D has increased. An increase in K_D from 11 to 35 μM reproduces this behavior (Fig. 12 G, G_2; Table I, G_2). Improved fits to R_{mod} were obtained with a slightly lower 30 μM K_D (unpublished data). However, a higher K_D provided better fits to ΔV_h (below).

The ΔV_h–Ca^{2+} relation for NEM is bell shaped (Fig. 12 H), consistent with an increase in K_D. The parame-

ters used to fit the R_{mod}–Ca^{2+} relation reproduce ΔV_h for $Ca^{2+} \geq 5$ μM, but greatly overestimate ΔV_h in 0 Ca^{2+}, reflecting the fivefold decrease in L_o (Fig. 12 H, G_2; Table I, G_2). This discrepancy can be accounted for, as with MTSES (Fig. 12 D), by increasing D to fit the 0 Ca^{2+} data and decreasing J_0 to improve the fit in high Ca^{2+} (Fig. 12 H, G_3; Table I, G_3).

Limitations of the Model and Data

The model incorporates several simplifying assumptions, including that Ca^{2+}-binding sites are identical. At $[Ca^{2+}]$ used in our experiments, contributions of low-affinity Mg^{2+}/Ca^{2+}-binding sites to channel gating are negligible (Shi and Cui, 2001; Zhang et al., 2001). However, recent studies suggest that BK channels may contain more than one high-affinity Ca^{2+}-binding site per subunit (Bao et al., 2002; Xia et al., 2002). Possible heterogeneity in binding sites should not affect our conclusion that cysteine modification strengthens the coupling between Ca^{2+} binding and channel opening and can also decrease binding affinity. However, the magnitude of changes in C and K_D could differ for each binding site. Selective effects of modifying reagents on different binding sites would certainly improve fits to R_{mod}– and ΔV_h–$[Ca^{2+}]$ relations owing to the increased number of free parameters. Multiple binding sites might help explain why the MTSET data sometimes changed over a narrower range of $[Ca^{2+}]$ than predicted by the model (Fig. 12 E). That being said, Scheme I, with a single type of binding site, was able to successfully reproduce that MTSES alters V_h only for $[Ca^{2+}] \leq 1$ μM and that MTSET leaves V_h unchanged over a narrow range of $[Ca^{2+}]$. These results together with the scatter in the data suggest that there is no compelling reason to increase the complexity of the model.

Relation to Previous Studies

Tang et al. (2004) recently identified C911 as an important target of oxidation in hSlo1. They found that channel modification by oxidation or cysteine-modifying reagents (MTSEA, MTSES, DNTB) produced similar inhibitory effects on steady-state activation at −20 mV in 4.7 μM Ca^{2+}. MTSEA had little effect on the G_K–V relation in 0 Ca^{2+} but reduced the ability of Ca^{2+} to shift the G–V. Mutation of C911 essentially eliminated this effect of MTSEA as well as the inhibitory effect of oxidation, consistent with the proposal that elimination of a free thiol at C911 inhibits Ca^{2+} binding to the nearby calcium bowl domain. A fast component of I_K inhibition by MTSEA was not eliminated by mutation of C911, consistent with the presence of additional modification-sensitive cysteines.

We observe effects of MTSET on K_D that are not eliminated by mutation of C430 or C615, and might therefore reflect modification of C911. An effect of C911 modification on K_D is consistent with the observations of Tang et al. (2004) However, several lines of evidence suggest that the contribution of C911 to our results is relatively small. First, mutants lacking C911 (C(18–29)A and C911A) still responded robustly to MTSET (Fig. 8 B), although the response exhibits an additional slow component that is not evident in the WT. Likewise C(18–29)A I_K is strongly inhibited by MTSES (Fig. 8 B). Moreover, the mutation C430A virtually abolishes the effects of MTSES in our experiments, suggesting either that C911 was not modified by MTSES or that its modification had no effect on gating. Tang et al. (2004) did not report whether effects of MTSES were prevented by mutation of C911, so it is possible that MTSES modification of C911 has no effect on function. Another possibility is that channels in our experiments are partially oxidized owing to an ∼30-min delay between patch excision and recording. Therefore, it is conceivable that modification of C911 was prevented by selective oxidation of this site. If C911 is oxidized to form a disulfide bond with another cysteine, then removal of C911 could expose the remaining disulfide partner to modification by MTSET, perhaps accounting for the additional slow component of MTSET action observed in mutants lacking C911.

Whether or not C911 is modified, our experiments identify additional modification-sensitive cysteines (C430, C615) and show that the functional consequences of their modification differ from those attributed to C911. In contrast to the effects of MTSEA reported by Tang et al. (2004), we find that cysteine modification alters steady-state activation in 0 Ca^{2+} as well as in the presence of Ca^{2+} and that effects may be inhibitory or excitatory depending on the modifying reagent, $[Ca^{2+}]$, and voltage. Differences in the effect of each reagent imply that modification of critical cysteines can be sensitive to the modifying adduct, not merely the absence of free thiol groups. For all reagents, we find that cysteine modification enhances the Ca^{2+}-dependent increase in $P_o(-120)$, whereas Tang et al. (2004) saw a decrease in the response to Ca^{2+} with MTSEA. We also observe effects on voltage-dependent gating even though there are no internally accessible cysteine residues in potential voltage-sensing domains (S2, S3, S4).

While we didn't study effects of oxidation, an interesting question is whether oxidation of C430 or C615 could alter BK channel function under pathophysiological conditions. An important feature of our results is that effects of cysteine modification are complex and can leave steady-state activation virtually unchanged over a range of $[Ca^{2+}]$ and voltage while producing marked changes in P_0 under different conditions. Therefore, demonstration by Tang et al. (2004) that mutation of C911 virtually eliminates the effect of oxidation on I_K in 4.7 μM Ca^{2+} at voltages near −20 mV

does not rule out that oxidation of additional sites effect P_0 under other conditions. Along these lines, it is worth noting that the effect of MTSET on mSlo1 was almost undetectable under conditions similar to those used by Tang et al. (2004) (e.g., −20 mV in 4.4 μM Ca^{2+}, Fig. 7 B), whereas significant changes in P_o were observed at more positive or negative voltages or in different $[Ca^{2+}]$.

Conclusions

Although the effects of MTSET, MTSES, and NEM on steady-state activation appear different, the above analysis suggests that their mechanisms of action are similar. MTSES and NEM both decrease the C-O equilibrium constant L_o fivefold. In all cases, modification of the WT channel is characterized by a 1.5–2-fold increase in the allosteric factor C, representing a 0.9–1.6 kCal/M increase in the energy of coupling between Ca^{2+} binding and channel opening. In addition, changes in voltage-dependent gating, in particular an increase in D (0.4–0.8 kCal/M), were required for all three reagents. Changes in the voltage sensor equilibrium constant (J_O) equivalent to a small 12–20-mV shift in the Q–V relation were also helpful in fitting the data, but had a relatively minor impact compared with L_o, C, and D. Most changes in L_o, C, and D produced by MTS reagents were abolished by the C430A mutation and can therefore be attributed to modification of this position. In addition, MTSET and NEM produce an approximate threefold increase in K_D. The effect of MTSET on K_D appears unaffected by C430A but is reduced by C615S. Thus, it is likely that MTSET and NEM reduce Ca^{2+} affinity by modifying C615 as well as additional cysteines. C615 lies in a high-affinity Haem-binding site, and the mutation C615S essentially eliminates the sensitivity of hSlo1 channels to inhibition by Heamin (Tang et al., 2003). Thus a role of C615 in regulating Ca^{2+} affinity could be relevant to the mechanism of Heamin action.

Differences in the effects of MTSET, MTSES, and NEM can be attributed primarily to differential effects on L_o and K_D. The ability of MTSET to shift the G–V in the opposite direction of MTSES or NEM is due primarily to the fivefold decrease in L_o produced by MTSES or NEM but not by MTSET. The marked decrease in $P_O(-120)$ produced by MTSET in intermediate $[Ca^{2+}]$ is caused by an increase in K_D that is not produced by MTSES. Thus, some effects of cysteine modification are dependent on the modifying adduct while others are not.

Although all reagents tested increased the coupling between Ca^{2+} binding and channel opening (C), it is significant that changes in C can occur independent of changes in L_0 and K_D. That is, MTSET increases C without altering L_0, and modification of C430 by any reagent increased C without altering K_D. In the allosteric model, C represents the ratio of K_Ds for the closed and open conformation ($C = K_D/K_{Dopen}$). Thus changes in a Ca^{2+}-binding site, which might be expected to perturb Ca^{2+} affinity for both closed and open conformations, would likely result in a change in K_D and possibly also in C. That C430 modification increases C without altering K_D is therefore consistent with a role of the C430 region in coupling that does not involve the Ca^{2+}-binding site but rather the linkage between binding site and gate. The relationship between C and L_0 is also relevant to the mechanism of linkage. For example, if the linkage acts to inhibit channel opening and is relieved by Ca^{2+} binding, then an increase in C might be expected to decrease the C-O equilibrium constant in 0 Ca^{2+} (L_0) without altering channel opening in saturating Ca^{2+}. This is exactly what we observe in response to MTSES modification (Fig. 12 C). However, a counter example is provided by MTSET, which increases channel opening in saturating Ca^{2+} without altering L_0. Thus, we cannot conclude whether the linkage between Ca binding and channel opening is inhibitory or excitatory, but suggest that understanding the difference between MTSET and MTSES action might prove relevant to addressing this question in the future.

It is remarkable that modification of a single site (C430) alters several aspects of gating and that the effect on L_o is dependent on the modifying adduct, whereas changes in C and D occur for all reagents. That C430 is located in the RCK1 domain may help explain the diversity of these effects on channel function. The RCK1 domain has been implicated in Ca^{2+}-dependent gating, where it is thought to play a role either in Ca^{2+} binding or in coupling the binding of Ca^{2+} to channel opening (Bao et al., 2002; Xia et al., 2002). In either case, the RCK1 domain must be linked to channel opening. Thus is reasonable that perturbations of the RCK1 domain could effect C (coupling) and L_o (channel opening). In addition, the ability of S4 mutations to inhibit Mg^{2+}-dependent activation suggests that interactions exist between RCK1 and the voltage sensor (Hu et al., 2003). Therefore, it is also reasonable that perturbations of the RCK1 domain could effect voltage-dependent gating (D, J_0).

The effects of C430 modification may reflect perturbation of interactions between the αD–βD linker and other parts of the channel. C430 is located within a sequence of eight amino acids in the αD–βD linker that is conserved in BK channels but absent from prokaryotic RCK domains. Thus, the structure of this region and its interactions with the rest of the channel are unknown. But it is likely that such interactions occur because the BK-specific residues are not required for the basic Rossmann-fold RCK structure, yet their deletion greatly enhances channel activation. It is possible that

interactions involving the αD–βD linker are electrostatic in nature because 4 out of 10 linker residues are charged, and COOH-terminal to C430, 4 out of 7 residues are negatively charged. Changes in electrostatic interactions might account for the different impact of positive (MTSET), negative (MTSES), and neutral (NEM) modifying adducts on L_o. The high negative charge density near C430 could also explain why modification by MTSET(+) is much more rapid than MTSES(−), although these reagents were applied at concentrations that produce similar reaction rates with neutral thiol compounds (Stauffer and Karlin, 1994).

Modification of C430 might also effect channel function by perturbing the nearby αD helix. In the MthK channel, αD helices in different RCK domains participate in a hydrophobic dimer interface that is involved in forming the RCK gating ring and thought to be important for transmitting Ca^{2+} binding to channel opening (Jiang et al., 2002). In addition, αD participates in a salt bridge with βE within the same RCK domain, disruption of which in hSlo1 alters channel function (Jiang et al., 2001). Thus, modification of C430 near αD might alter BK channel function by perturbing the RCK1–RCK2 interaction and/or the αD–βE salt bridge.

Finally, another feature of the RCK1 domain that may be relevant to the broad effects of C430 modification on gating is its mechanical properties. Niu et al. (2004) found that reductions in the length of the S6–RCK1 linker increase open probability in the presence or absence of Ca^{2+}, and concluded that the S6–RCK1 linker and the RCK gating ring have spring-like properties that exert tension on the S6 gate and govern open probability. They also proposed that most of the spring is in the gating ring. Consistent with this hypothesis, we find that deletion of the RCK1 αD–βD linker shifts the G–V relations in both 0 and 70 μM Ca^{2+} to more negative voltages similar to the effect of shortening the S6–RCK1 linker. If modification of C430 alters the mechanical properties of the gating ring, then it could potentially impact multiple features of gating by altering the transduction of local conformational changes in the COOH-terminal tail domain into changes in channel opening.

This work was supported in part by a grant from the National Institutes of Health (NS42901) for F.T. Horrigan.

Olaf S. Andersen served as editor.

Submitted: 13 July 2004
Accepted: 21 December 2004

REFERENCES

Adelman, J.P., K.Z. Shen, M.P. Kavanaugh, R.A. Warren, Y.N. Wu, A. Lagrutta, C.T. Bond, and R.A. North. 1992. Calcium-activated potassium channels expressed from cloned complementary DNAs. *Neuron.* 9:209–216.

Armstrong, C.M., and F. Bezanilla. 1974. Charge movement associated with the opening and closing of the activation gates of the Na channels. *J. Gen. Physiol.* 63:533–552.

Avdonin, V., X.D. Tang, and T. Hoshi. 2003. Stimulatory action of internal protons on Slo1 BK channels. *Biophys. J.* 84:2969–2980.

Bao, L., A.M. Rapin, E.C. Holmstrand, and D.H. Cox. 2002. Elimination of the BK(Ca) channel's high-affinity Ca^{2+} sensitivity. *J. Gen. Physiol.* 120:173–189.

Bao, L., C. Kaldany, E.C. Holmstrand, and D.H. Cox. 2004. Mapping the BKCa channel's "Ca^{2+} bowl": side-chains essential for Ca^{2+} sensing. *J. Gen. Physiol.* 123:475–489.

Brenner, R., T.J. Jegla, A. Wickenden, Y. Liu, and R.W. Aldrich. 2000. Cloning and functional characterization of novel large conductance calcium-activated potassium channel β subunits, hKCNMB3 and hKCNMB4. *J. Biol. Chem.* 275:6453–6461.

Butler, A., S. Tsunoda, D.P. McCobb, A. Wei, and L. Salkoff. 1993. mSlo, a complex mouse gene encoding "maxi" calcium-activated potassium channels. *Science.* 261:221–224.

Cox, D.H., J. Cui, and R.W. Aldrich. 1997a. Allosteric gating of a large conductance Ca-activated K^+ channel. *J. Gen. Physiol.* 110: 257–281.

Cox, D.H., J. Cui, and R.W. Aldrich. 1997b. Separation of gating properties from permeation and block in mslo large conductance Ca-activated K^+ channels. *J. Gen. Physiol.* 109:633–646.

Cui, J., and R.W. Aldrich. 2000. Allosteric linkage between voltage and Ca^{2+}-dependent activation of BK-type mslo1 K^+ channels. *Biochemistry.* 39:15612–15619.

Cui, J., D.H. Cox, and R.W. Aldrich. 1997. Intrinsic voltage dependence and Ca^{2+} regulation of mslo large conductance Ca-activated K^+ channels. *J. Gen. Physiol.* 109:647–673.

Diaz, F., M. Wallner, E. Stefani, L. Toro, and R. Latorre. 1996. Interaction of internal Ba^{2+} with a cloned Ca^{2+}-dependent K^+ (hslo) channel from smooth muscle. *J. Gen. Physiol.* 107:399–407.

DiChiara, T.J., and P.H. Reinhart. 1997. Redox modulation of hslo Ca^{2+}-activated K^+ channels. *J. Neurosci.* 17:4942–4955.

Erxleben, C., A.L. Everhart, C. Romeo, H. Florance, M.B. Bauer, D.A. Alcorta, S. Rossie, M.J. Shipston, and D.L. Armstrong. 2002. Interacting effects of N-terminal variation and strex exon splicing on slo potassium channel regulation by calcium, phosphorylation, and oxidation. *J. Biol. Chem.* 277:27045–27052.

Hamill, O.P., A. Marty, E. Neher, B. Sakmann, and F.J. Sigworth. 1981. Improved patch-clamp techniques for high-resolution current recording from cells and cell-free membrane patches. *Pflugers. Arch.* 391:85–100.

Herrington, J., and R.J. Bookman. 1995. Pulse Control. University of Miami Press, Miami.

Horrigan, F.T., and R.W. Aldrich. 1999. Allosteric voltage gating of potassium channels II. Mslo channel gating charge movement in the absence of Ca^{2+}. *J. Gen. Physiol.* 114:305–336.

Horrigan, F.T., and R.W. Aldrich. 2002. Coupling between voltage sensor activation, Ca^{2+} binding and channel opening in large conductance (BK) potassium channels. *J. Gen. Physiol.* 120:267–305.

Horrigan, F.T., J. Cui, and R.W. Aldrich. 1999. Allosteric voltage gating of potassium channels I. Mslo ionic currents in the absence of Ca^{2+}. *J. Gen. Physiol.* 114:277–304.

Hu, L., J. Shi, Z. Ma, G. Krishnamoorthy, F. Sieling, G. Zhang, F.T. Horrigan, and J. Cui. 2003. Participation of the S4 voltage sensor in the Mg^{2+}-dependent activation of large conductance (BK) K^+ channels. *Proc. Natl. Acad. Sci. USA.* 100:10488–10493.

Jiang, Y., A. Pico, M. Cadene, B.T. Chait, and R. MacKinnon. 2001. Structure of the RCK domain from the *E. coli* K^+ channel and demonstration of its presence in the human BK channel. *Neuron.* 29:593–601.

Jiang, Y., A. Lee, J. Chen, M. Cadene, B.T. Chait, and R. MacKinnon. 2002. Crystal structure and mechanism of a calcium-gated potassium channel. *Nature.* 417:515–522.

Kehl, S.J. 1996. Block of BK (maxi K) channels of rat pituitary melanotrophs by Na^+ and other alkali metal ions. *Pflugers. Arch.* 432: 623–629.

Meera, P., M. Wallner, M. Song, and L. Toro. 1997. Large conductance voltage- and calcium-dependent K^+ channel, a distinct member of voltage-dependent ion channels with seven N-terminal transmembrane segments (S0-S6), an extracellular N terminus, and an intracellular (S9-S10) C terminus. *Proc. Natl. Acad. Sci. USA.* 94:14066–14071.

Morales, E., W.C. Cole, C.V. Remillard, and N. Leblane. 1996. Block of large conductance Ca^{2+}-activated K^+ channels in rabbit vascular myocytes by internal Mg^{2+} and Na^+. *J. Physiol.* 495:701–716.

Neyton, J. 1996. A Ba^{2+} chelator suppresses long shut events in fully activated high-conductance Ca^{2+}-dependent K^+ channels. *Biophys. J.* 71:220–226.

Niu, X., X. Qian, and K.L. Magleby. 2004. Linker-gating ring complex as passive spring and Ca^{2+}-dependent machine for a voltage- and Ca^{2+}-activated potassium channel. *Neuron.* 42:745–756.

Qian, X., C.M. Nimigean, X. Niu, B.L. Moss, and K.L. Magleby. 2002. Slo1 tail domains, but not the Ca^{2+} bowl, are required for the β1 subunit to increase the apparent Ca^{2+} sensitivity of BK channels. *J. Gen. Physiol.* 120:829–843.

Rothberg, B.S., and K.L. Magleby. 1999. Gating kinetics of single large-conductance Ca^{2+}-activated K^+ channels in high Ca^{2+} suggest a two-tiered allosteric gating mechanism. *J. Gen. Physiol.* 114: 93–124.

Rothberg, B.S., and K.L. Magleby. 2000. Voltage and Ca^{2+} activation of single large-conductance Ca^{2+}-activated K^+ channels described by a two-tiered allosteric gating mechanism. *J. Gen. Physiol.* 116:75–99.

Schreiber, M., and L. Salkoff. 1997. A novel calcium-sensing domain in the BK channel. *Biophys. J.* 73:1355–1363.

Schreiber, M., A. Yuan, and L. Salkoff. 1999. Transplantable sites confer calcium sensitivity to BK channels. *Nat. Neurosci.* 2:416–421.

Schubert, R., and M.T. Nelson. 2001. Protein kinases: tuners of the BKCa channel in smooth muscle. *Trends Pharmacol. Sci.* 22:505–512.

Shi, J., and J. Cui. 2001. Intracellular Mg^{2+} enhances the function of BK-type Ca^{2+}-activated K^+ channels. *J. Gen. Physiol.* 118:589–606.

Shi, J., G. Krishnamoorthy, Y. Yang, L. Hu, N. Chaturvedi, D. Harilal, J. Qin, and J. Cui. 2002. Mechanism of magnesium activation of calcium-activated potassium channels. *Nature.* 418:876–880.

Stauffer, D.A., and A. Karlin. 1994. Electrostatic potential of the acetylcholine binding sites in the nicotinic receptor probed by reactions of binding-site cysteines with charged methanethiosulfonates. *Biochemistry.* 33:6840–6849.

Stefani, E., M. Ottolia, F. Noceti, R. Olcese, M. Wallner, R. Latorre, and L. Toro. 1997. Voltage-controlled gating in a large conductance Ca^{2+}-sensitive K^+ channel (hslo). *Proc. Natl. Acad. Sci. USA.* 94:5427–5431.

Tang, X.D., H. Daggett, M. Hanner, M.L. Garcia, O.B. McManus, N. Brot, H. Weissbach, S.H. Heinemann, and T. Hoshi. 2001. Oxidative regulation of large conductance calcium-activated potassium channels. *J. Gen. Physiol.* 117:253–274.

Tang, X.D., R. Xu, M.F. Reynolds, M.L. Garcia, S.H. Heinemann, and T. Hoshi. 2003. Haem can bind to and inhibit mammalian calcium-dependent Slo1 BK channels. *Nature.* 425:531–535.

Tang, X.D., M.L. Garcia, S.H. Heinemann, and T. Hoshi. 2004. Reactive oxygen species impair Slo1 BK channel function by altering cysteine-mediated calcium sensing. *Nat. Struct. Mol. Biol.* 11: 171–178.

Tseng-Crank, J., C.D. Foster, J.D. Krause, R. Mertz, N. Godinot, T.J. DiChiara, and P.H. Reinhart. 1994. Cloning, expression, and distribution of functionally distinct Ca^{2+}-activated K+ channel isoforms from human brain. *Neuron.* 13:1315–1330.

Xia, X.M., X. Zeng, and C.J. Lingle. 2002. Multiple regulatory sites in large-conductance calcium-activated potassium channels. *Nature.* 418:880–884.

Zhang, X., C.R. Solaro, and C.J. Lingle. 2001. Allosteric regulation of BK channel gating by Ca^{2+} and Mg^{2+} through a nonselective, low affinity divalent cation site. *J. Gen. Physiol.* 118:607–636.